Effects of Thermal Ageing on Mechanical Property and Microstructure for Reduced Activation Ferritic/Martensitic Steels

LI, Yanfen

Doctor of Philosophy

Department of Fusion Science

School of Physical Sciences

The Graduate University for Advanced Studies

2009

CONTENTS

ABSTRACT

Blanket is one of the key components of fusion reactors, which provides the main heat transfer and tritium breeding systems. Currently, reduced activation ferritic/martensitic steels (RAFMs) are considered as the primary candidates for blanket structural materials because of their most matured technological base and good irradiation resistance. In the past two decades, several advanced RAFM steels have been developed with continuous improvements in the world. Among these, JLF-1 steel is a Japanese candidate, and CLAM steel is a Chinese reference.

In fusion reactor application, the structural materials will be exposed to long-term loading at high temperature, which may result in the changes of mechanical property and microstructure. The thermal changes of property and microstructure at the operation temperature are called ageing. Thermal ageing may reduce the maximum operation temperature by reduction of yield strength and/or creep strength. However, up to now, the understanding of the ageing effects is not sufficient. The objectives of this work are: (1) to investigate the thermal ageing effects on mechanical properties changes, including hardness, tensile and creep deformation, (2) to clarify mechanism of the mechanical property changes by correlation with microstructural evolution, and (3) to apply the experimental data obtained to the blanket design.

In this study, the JLF-1 (JOYO-II-HEAT) and CLAM (0603 HEAT) were used for comparison. The chemical compositions (in weight%) were 9.00 Cr, 1.98 W, 0.49 Mn, 0.20 V, 0.083 Ta, 0.09 C, and balance Fe for JLF-1, and 8.94 Cr, 1.45 W, 0.44 Mn, 0.19 V, 0.15 Ta, 0.13 C, and balance Fe for CLAM. Thus, CLAM has higher level of Ta and lower level of W than those of JLF-1. The heat treatments included the normalization (1323 K/60 minutes for JLF-1 and 1253 K/30 minutes for CLAM) and tempering (1053 K/60 minutes for JLF-1 and 1033 K/90 minutes for CLAM). By comparing the two alloys, the effects of the composition and the heat treatment were investigated.

The thermal ageing experiments were carried out at a temperature range from 823 to 973 K up to 2000 h and under high vacuum to prevent oxidation. The temperature of 823 K was chosen to simulate the typical upper limit temperature for fusion reactor, and 973 K was chosen to accelerate the thermal processes. The mechanical properties including the hardness, tensile and creep were tested. Microstructural evolution was examined by Scanning Electron Microscope (SEM) and Transmission Electron Microscope (TEM) equipped with Energy Dispersive Spectrometer (EDS).

The results showed that, the hardness increased slightly after ageing at 823 K for 100 and 2000h for the both steels, suggesting ageing-induced hardening. However, the hardness decreased at

873K and above, indicating ageing-induced softening. No significant changes were detected in both yield strength and ultimate tensile strength after ageing at 823 K for 2000 h, while the strength decreased after higher temperatures ageing.

The creep curves of the both steels, similar to other RAFM steels, exhibited three regions: the short primary creep, the secondary creep which was a linear process with a minimum creep rate, and the tertiary characterized by an increased creep rate with time. After ageing at 823 and 873 K for 2000 h, the creep property improved. However, it degraded significantly after ageing at 973K for 100 h.

JLF-1 and CLAM steels before ageing exhibited a mixture of martensitic lath and tempered martensitic structure with two types of precipitates, $M_{23}C_6$ and TaC. Microstructural evolution revealed that, the number density of small precipitates (< 80 nm) increased significantly after ageing from 823 to 923 K up to 2000 h. However, after ageing at 973 K for 100 h, the density of small precipitates decreased, and the recovery of microstructure partially was also observed. By analysis of the chemical composition using EDS, most of the small precipitates were identified to be Ta-rich carbide (TaC), and the larger precipitates to be the Cr-rich carbide ($M_{23}C_6$).

A traditional dispersed obstacle model was used to correlate the hardness change and the microstructure. In this model, the dominant obstacle was assumed to be precipitates only. The typical hardening (823K/2000h) and softening (973K/100h) conditions were chosen for calculation. The results showed that the calculated hardness change almost agreed with the measured ones after ageing at 823 K for 2000 h, suggesting that the new formation of TaC was responsible for the hardening. However, there is a large difference between the calculated and measured dada after ageing at 973 K for 100 h, indicating that the loss of TaC alone cannot account for the softening. The recovery of lath structure and dislocations would contribute the major effects to the softening.

Comparing the two steels, the CLAM has higher hardness and tensile strength, smaller minimum creep rate and longer rupture time than those of JLF-1, while the susceptibility to thermal ageing of CLAM was larger than that of JLF-1. The lower normalization and tempering temperature and higher level of Ta were considered to be responsible for the finer grain and smaller martensitic lath width, thus leading to the higher hardness and strength for CLAM than those of JLF-1. However, the study showed that, because of the lower heat treatment temperature, the CLAM was more susceptible to thermal ageing, suggesting that the present heat treatment condition is not the best one. Increase in heat treatment temperature is necessary to improve the stability to thermal ageing for CLAM.

Since testing materials for the actual operation time is extremely costly and time-consuming,

prediction of creep rupture performance in blanket conditions is critically important. In this work, the Larson-Miller parameter was used for prediction, which was based on the results of short-term creep experiments at higher temperatures with higher stresses. By prediction, the rupture stress at the typical blanket condition, 823 K for 100 000h, was estimated to be about 140 MPa for the both steels, and the present prior ageing influenced the rupture stress by about ± 10 MPa. This result can provide a reference for the design of fusion blanket.

In summary, this study has demonstrated the effects of thermal ageing on mechanical property and microstructural evolution for JLF-1 and CLAM steels. One of the important new findings is that the TaC is unstable, which can form newly or disappear by dissolution during the ageing. Ta is an element newly used in RAFM steels, instead of Nb in the conventional steel for the purpose of avoiding long radioactivity. Thus limited understanding of the status of Ta has been available up to now. The present study showed that the future control of TaC can enhance the thermal properties of RAFM steels. Since the Larson-Miller parameter only included partial effects of property change by ageing, the LMP correlated with pre-aged experiments in this study can provide the suggestion for developing suitable methods to predict the creep performance in blanket conditions including the overall ageing effects.

CHAPTER 1

Introduction

1.1Energy issue and fusion reactor

1.1.1 Energy development in the world

Generally, the energy sources in the world can be classified into two groups: renewable and non-renewable energy sources.

Petroleum, natural gas and coal are known as fossil fuels or mineral fuels and are non-renewable energy sources formed more than 300 million years ago. With the development of society and economy, human beings began to consume the resources on a large scale. Fossil fuels account for about 80% of the primary energy consumption at present [1]. However, so far about half of the reserves have been depleted. It was predicted that the reserves would be totally depleted in several decades at our present rate of use [2].

In addition, fossil fuels are the source with many problems difficult to resolve, such as environmental degradation at the local, regional and global level. Burning fossil fuels to get energy causes air pollution, acid rain and produce CO_2. The release of CO_2 causes a critical environmental issue of "green house effect", which increases global warming and may cause more critical issues of abominable global climate [3].

The renewable energy sources include modern biomass, wind, solar, marine and geothermal energy, which merely represent 4.4% of the energy consumption [4]. However they are unstable in nature because they are subjected to climatic change, and require complex management of the electricity supply network or the additional cost for accompanying energy storage. They can make a large contribution in countries with a distributed population and lack of electricity network, but they can only cover a minor part of the energy demands at those locations where developed nations currently live.

Nuclear energy is one of the new energy sources. In the past, nuclear energy based on fission has been adopted by many developed and the most advanced developing countries [5]. Technically, the ability to deploy fission as a long-term energy source has been demonstrated. A number of countries consider fission as a vital element in their current and future electricity supply. Clearly, having developed the technology and the infrastructure of its management, it is likely that fission will continue to have a future role alongside other electricity supply alternatives. However, the non-breeding fission fuels also will be depleted in the near future.

Nowadays with the rapid development of economy, society and population, the demand of human being for energy is remarkably increased. The globe will be faced the energy crisis. Thus, the development of a long-term, huge and new energy source is becoming one of the critical issues.

1.1.2 The role of fusion energy

Considerable efforts are being expended worldwide to develop a long-term energy source. Nuclear fusion is considered as an attractive and possible solution for energy crisis, which can offer the potential of an almost limitless source of energy for future generations. Similar to the process that powers the sun and stars, nuclear fusion is a reaction of light atoms with other light atoms and making heavier atoms and huge energy [6].

Fusion energy has the special advantages as follows [7, 8]:

(1) Fusion energy has an almost limitless fuel supply.

The basic fuels are distributed widely on earth and are essentially inexhaustible. Deuterium is abundant and can be extracted easily from sea water. Tritium can be produced from lithium, and lithium is a readily available light metal in the Earth's crust. Unlike other natural sources, these fuels are available worldwide.

(2) Fusion energy is a clean energy.

Waste from fission is a long-term burden for future generations. But for fusion, by careful selection of low-activation structural materials, the radioactivity will reach an acceptable level after several decades recycle or disposal.

(3) Fusion is a safe energy.

Unlike fission, in which chain reactions are used in the power plants, fusion uses one-through reaction. So the fusion reaction can be stopped rapidly by stopping fuel supply.

1.1.3 Fusion reactor

The most suitable fusion reaction occurs between the nuclei of the two heavy isotopes of hydrogen, deuterium (D) and tritium (T), to form a helium nucleus and release of a neutron and energy [9], as shown in *equation 1-1* and *Fig. 1-1*.

$$^{2}D + {}^{3}T \rightarrow {}^{4}He\ (3.5\ MeV) + {}^{1}n\ (14.1\ MeV) + Energy \qquad (1\text{-}1)$$

There are mainly two ways to achieve controlled fusion reactors to produce electric power on earth, namely inertial confinement fusion (ICF) and magnetic confinement fusion (MCF) [10].

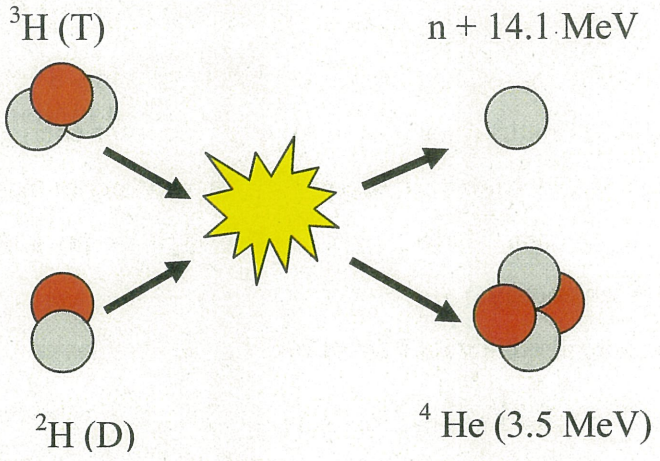

Fig.1-1 Schematic illustration of D-T fusion reaction

ICF is a process where nuclear fusion reactions are initiated by heating and compressing a fuel target, typically in the form of a pellet that most often contains a mixture of D and T [10]. The aim of ICF is to produce a condition known as "ignition", where this heating process causes a chain reaction that burns a significant portion of the fuel. To date most of the work in ICF for energy purpose has been carried out in the United States, European Union and Japan, and generally has seen less development effort than magnetic approaches.

MCF is an approach to confine the fusion fuel in the form of plasma by using magnetic fields [10]. MCF is more highly developed and usually considered more promising for energy production. One of the promising MCF confinements is tokamak concept [11], which is studied as the dominate concept in the world. Stellarator is another concept, such as the helical-type device [11].

Now a tokamak-type International Thermonuclear Experimental Reactor (ITER) is under construction [9]. ITER device is just an experimental reactor, as shown in *Fig.1-2*. The ultimate goals of ITER are to demonstrate ignition and extended burns of D-T plasmas with steady-state, and serve as a test facility for advanced components such as blankets.

The production of net electrical power from fusion is planned for demonstration reactor (DEMO) [12], the next generation experiment after ITER. In DEMO, all reactor-relevant functions like the breeding of tritium or the successful operation of a divertor have to be demonstrated and successfully tested.

Nowadays, several conceptual designs of tokamak-type DEMO reactors are proposed and carried out, such as SSTR in USA [13], ARIES [14], and FDS-II [15] in China, and so on. Helical-type DEMO reactor is another design concept in National Institute for Fusion Science (NIFS) in Japan, which is based on the experience of LHD device, as shown in *Fig. 1-3*.

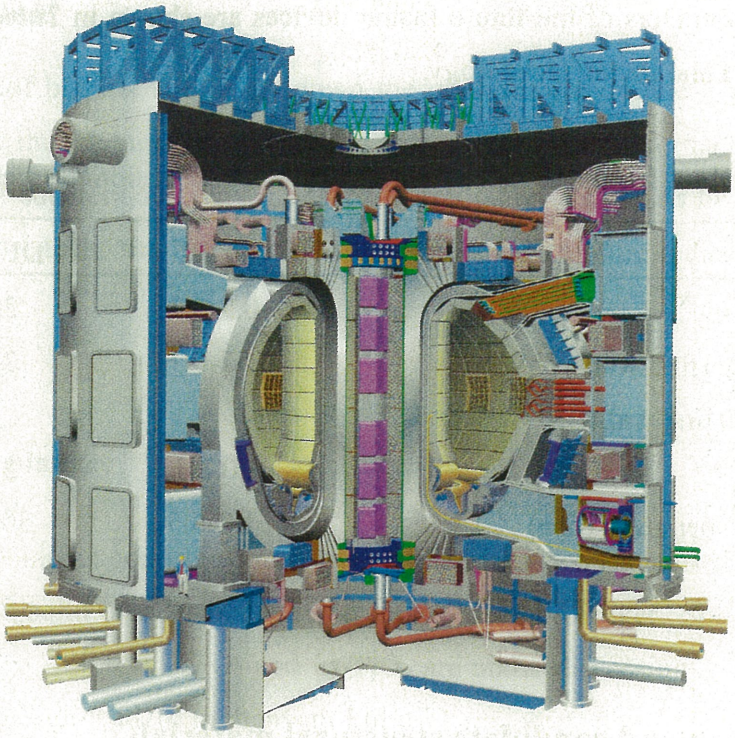

Fig. 1-2 The tokamak-type International Thermonuclear Experimental Reactor (ITER) device [9]

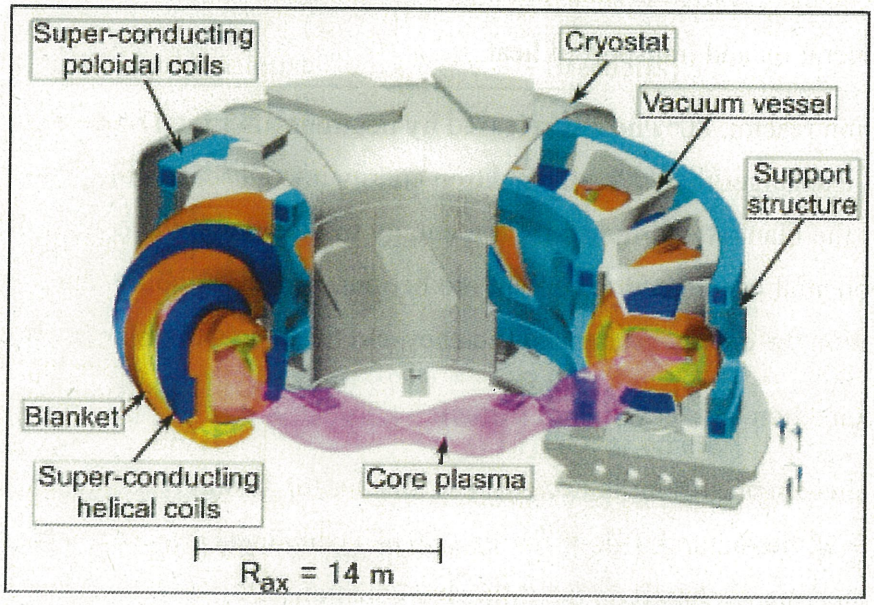

Fig. 1-3 The 3-D illustration of the FFHR2m1, the Helical-type DEMO reactor [16]

The general parameters of the future fusion devices are shown in *Table 1-1* based on present knowledge in plasma and fusion technology.

Table 1-1 General performance parameters of fusion devices [17]

	ITER	DEMO	REACTOR
Fusion Power, GW	0.5-0.7	2-4	3-4
Neutron wall loading (first wall), MW/m^2	0.57-0.78	2-3	2-3
Integrated wall load (first wall)			
In MWy/m^2	~0.3-1	3-8	10-15
In displacements per atom (dpa)	1.7-5.5	30-80	100-150
Operation mode	pulsed	Quasi-continuous	

1.2 Blanket system and candidate structural materials

1.2.1 The role and functions of blanket

Blanket is one of the important components in fusion reactors and located between the plasma and vacuum vessel. The blanket consists of breeder, coolant and neutron multiplier. The main functions of blanket are listed as followed [18-19]:

(1) The generation and transport of heat

In real fusion reactor, 80% heat is released by neutrons after the D-T reaction. The blanket is basically a heat exchanger to convert the neutron energy into a useful form of thermal energy.

To protect the blanket and transform the energy to electricity, the coolant is involved in the blanket. The potential candidates of coolant are helium, water or liquid metal, etc. The choice of coolant depends on the energy exchange efficiency and the concept of blanket design.

(2) The production and recycling of tritium

As the fuel element, tritium is necessary to sustain the fusion reaction. There is abundant D on earth. However, the natural T does not exist. The economical way is to generate T during the operation of fusion reactor based on the following equations [20]:

$$^{6}Li + n \rightarrow {}^{4}He + T + 4.78MeV \qquad (1\text{-}2)$$

$$^{7}Li + n \rightarrow {}^{4}He + T + n - 2.4MeV \qquad (1\text{-}3)$$

(3) The neutron shield

Another function of blanket is to slow down the neutrons and protect the vessel and other components, especially the magnet. The irradiation with neutrons heats up the coil of magnet and results in the failure of superconductivity. Long time irradiation also leads to the degradation of superconductivity, and reduces the life time of structural and insulating materials of the magnet system.

1.2.2 The category of blanket

All of the DEMO blanket concepts could be classified into two categories with regard to the breeding materials [21]: solid breeder blanket and liquid breeder blanket. Solid ceramic breeder materials, such as Li_2O, Li_4SiO_4, Li_2ZrO_3 and Li_2TiO_3 are under discussion, while liquid breeder materials are lithium, lithium-lead, or molten-salt Flibe.

Within the framework of the ITER, the seven ITER Parties have made several proposals for DEMO-relevant Test Blanket Modules (TBMs) to be tested in ITER from the first day of H-H operation [9]. The tests of TBMs in ITER will give essential information to accomplish breeding blanket development for DEMO. The *Table l-2* lists the design of liquid breeding blanket concepts.

Table 1-2 TBM designs using liquid breeding materials [22]

TBM type	Structural materisl	Breeder(s)	Coolant
China HCSB	EUROFER	Li_4SiO_4	He
EU HCSB	EUROFER	Li_4SiO_4 or Li_2TiO_3	He
Japan HCSB	F82H	Li_2TiO_3 or others	He
Korea HCSB	EUROFER	Li_4SiO_4	He
RF HCSB	FS (9CrMoVNb)	Li_4SiO_4	He
US HCSB	F82H or EUROFER	Li_4SiO_4 or Li_2TiO_3	He
Japan WCSB	F82H	Li_2TiO_3 or others	H_2O
China DFLL	CLAM	Pb-17Li (also as partial coolant)	He
EU HCLL	EUROFER	Pb-17Li	He
US DCLL	F82H	Pb-17Li (also as partial coolant)	He
Korea HCML	EUROFER	Li	He
RF SCLi	V-4Cr-4Ti	Li (also as partial coolant)	

1.2.3 Requirement to structural materials of blanket

The blanket systems are large systems with combined thermal, hydraulic and mechanical loading, irradiation, corrosion etc. The structural materials are the main concern and one of most severely exposed parts of blanket. Development of structural materials plays a key role for the successful implementation of fusion reactors [23].

The requirements to structural materials are arguably strict. Besides the basic physical, chemical and mechanical properties, the materials are needed to be satisfied the following requirements:

(1) Low activation

Low activation is a quite attractive factor of fusion reactor. The material should be of low activation in order to reduce the potential risk related to accidents, facilitate the maintenance operation and simplify the decommissioning and waste management.

Different from fission reactors, no high level radioactive nuclides will be produced from fusion reactors. By careful selection of the alloy elements, the amount of long half-life radioactivity of the structural materials should be reduced to the point that the materials can be recycled or reused after about several decades [24].

(2) Good resistance to neutron irradiation

The fusion reactor will produce 14.1 MeV high-energy neutrons. These strong neutrons can produce serious irradiation damage on structural materials, leading to the microstructure and mechanical property changes, such as the sharp increase in yield strength at lower temperature irradiation region and thus resulting in upward shift of the ductile-brittle transition temperature (DBTT) [25], He embrittlement at relatively high temperature [26], and so on. Therefore, a good resistance to neutron irradiation is essential.

(3) High thermo-physical and mechanical properties at high temperature

The structural material will suffer from complex thermo-mechanical loading which is caused by high surface heat flux, electromagnetic loading and alternating thermal stresses [27]. Therefore, a combination of good mechanical strength, low coefficient of thermal expansion and high thermal conductivity at high temperatures is necessary.

What's more, high operation temperatures will provide the energy conversion efficiency to cope with the competing sources in the future energy market.

(4) Good compatibility with coolant and breeder/neutron multiplier

The compatibility of materials is another issue and has to be taken into account, which includes corrosion, chemical interactions, coolant systems pressure and coolant/breeder temperature constraints [28-30].

(5) Long service life

The lifetime of structural material must be long enough to minimize the necessary replacements of near-plasma components.

1.2.4 Candidate structural materials

As discussed above, low activation materials must be used to maintain the good environmental benignity of fusion energy. Only a few of elements have acceptable radiological safety performance and low long-term radiation levels. The most promising elements are V, Cr, Ti, C, Si, Fe, Mn, etc.. However, cares must be taken to control the impurities of high long-term radioactivity, such as Ag, Bi, Nb and Mo, to several wppm [31-32].

Three major structural materials which can fulfil the requirement of "low activation" have been considered [33-35]: reduced activation ferritic/martensitic steels (RAFMs), vanadium alloys and SiC/SiC composites. These three material groups are pursued in national and international materials R&D programs and considered as the candidates structural materials in different design concepts for DEMO blanket in the world.

(1) RAFM steels

RAFM steels are a modified composition of conventional Fe-(8-12)Cr-(1-2)Mo steels by exchanging Mo, Ni and Nb with W, V and Ta for the purpose of obtaining low activation characteristics. They have the most matured technological base relative to other candidate materials, good resistance to neutron irradiation. The detail about the RAFM steels will be reported in the next section.

(2) Vanadium alloy

Vanadium alloys were initially investigated and developed in the 1960s and 1970s for use as fuel cladding in the liquid metal reactor programs [36]. Because of their low activation

characteristics coupled with high-temperature strength and high thermal stress factor, V alloys are considered to be the attractive candidate materials for fusion reactors.

Extensive research and development has resulted in a significant progress. The emphasis of the worldwide V alloy development effort has been on the V-Cr-Ti system [37]. These three elements all exhibit the favorable low-activation characteristics. The addition of a few percent Ti has been proved to enhance resistance to irradiation-induced swelling, thus offering a potential for long operation lifetime in fusion reactors. In addition, a few percent Cr can significantly improve the tensile and creep strength of V-Ti alloys.

Currently, the V-4Cr-4Ti is considered to be a reference alloy in many research programs. Several large heats of V-4Cr-4Ti were produced in the US [37], Japan [38] and Russia [39], followed by fabrication of products such as thin and thick plates, rods and wires, and tubes and weld joints. In Japan, NIFS-HEAT-1 and NIFS-HEAT-2 were fabricated by NIFS with low oxygen levels [40]. In Southwestern Institute of Physics (SWIP) in China, several small ingots of V-4Cr-4Ti were produced [41]. Through these efforts, fabrication technology for V alloys has been remarkably advanced.

However, a number of critical issues are remaining and these problems should be resolved before the practical application in the future, such as the high susceptibility to impurities elements of O, N and H, low temperature irradiation embrittlement, and so on. In addition, the data base of V alloys is limited.

(3) SiC/SiC Composites

SiC composites were initially developed for aerospace and fossil energy applications, because of their most important properties of high temperature strength, strength to weight ratio, and corrosion resistance [42-43]. For fusion applications, interest in this material is not only from its low activation property but also from its mechanical strength at very high temperature (to 1000°C).

Research on SiC composites for fusion applications has focused on the effects of irradiation on dimensional stability, strength, and thermal conductivity [44-45]. There are significant improvements in radiation resistance of SiC/SiC and in understanding radiation effect mechanisms [46]. However, Development of SiC/SiC composites for fusion must be considered to be in the very early stages with many scientific and engineering hurdles to overcome.

Some comparisons of these three candidate materials are summarized in *Table 1-3*.

Table 1-3 Development status of low activation structural materials [47]

Category	RAFM steels	V alloy	SiC/SiC
Industrial base	Large	Small	Small
Data base			
Unirradiated	Large	Moderate	Small
Irradiated	Large	Small	Very small
Fabrication experience	Large	Small	Very small
Test standards	Yes	Yes	Partial
ASME design code development	Yes	Yes	

1.3 The R & D of RAFM steels

1.3.1 History of RAFM steels development

RAFM steels have the most advanced technology base of the three materials and a promising irradiation performance. Presently, they are considered as the primary candidates for fusion blanket structural materials.

Ferritic steels were considered as structural materials for fusion reactors in the late 1970s. The first ferritic steels considered in the USA program were Sandvik HT9 (nominally 12Cr-1Mo-0.25V-0.5W-0.5Ni-0.2C, usually designated 12Cr-1MoVW) [48] and modified 9Cr-1Mo steel (9Cr-1Mo-0.2V-0.06Nb-0.1C, designated 9Cr-1MoVNb) [49]. Similarly, the first steels in the programs in Europe and Japan were the steels previously considered in their fast reactor programs, such as EM-12, FV448, DIN1.4914, and JFMS [35].

In the mid-1980s, the idea of low-activation materials was introduced into the international fusion programs. Therefore, fusion reactor materials research programs in Japan, the European Union, and the United States began working toward developing RAFM steels.

The Cr-V and Cr-W-V systems steels were mainly developed under these fusion materials programs. The principal approaches adopted in this development are [50]: (a) the replacement of the radiologically undesirable Mo, Nb, and Ni in the existing commercial steels by elements such as W, V, Ta and Mn, which have equivalent or similar effects on the constitution and structures, and (b) the removal of the impurities that adversely influence the induced activities and dose rates when present in low concentrations in the steels.

Ferritic steels with 12% Cr were considered, which were basically developed for fossil boiler

and steam generator applications and were investigated for use as cladding and duct materials in liquid metal reactors (LMR) [35]. However, it is difficult to eliminate the δ-ferrite, which can cause low toughness and high embrittlement. At the same time, low Cr steels (2.25%Cr) were also studied and considered [35]. But in the end, 7-9% Cr steels were chosen for further study and development because [51]:

(1) Production and fabrication of 7~10%Cr steels are well qualified with established industrial processes.

(2) The 7~10%Cr steels show promising phase stability, resistance to temper embrittlement, good weldability, etc.

(3) The 7~10%Cr steels have shown the best irradiation resistance of the steels.

The nominal compositions of several advanced RAFM steels including the impurity elements are summarized in *Table 1-4*, which were investigated in the USA, European, Japanese, and Chinese fusion materials programs.

Table 1-4 Typical compositions and proposed specifications for RAFMs [51,52]

Elements	ORNL 9Cr-2WVTa	F82H	F82H-IEA	JLF-1	EUROFER 97	CLAM
Cr	8.5-9.0	8.0	7.5-8.5	9.0	8.0-9.0	8.5-9.5
C	0.1	0.1	0.08-0.12	0.1	0.10-0.12	0.08-0.12
W	2.0	2.0	1.8-2.2	2.0	1.0-1.2	1.4-1.6
V	0.25	0.2	0.15-0.25	0.19	0.20-0.30	0.15-0.30
Ta	0.07	0.04	0.01-0.06	0.07	0.06-0.10	0.13-0.17
Mn	0.45	0.5	<0.5	0.45	0.4-0.6	0.4-0.6
P	-	<0.02	<0.01	-	<0.0005	<0.0005
S	-	<0.01	<0.01	-	<0.005	<0.0005
B	-	0.003	<0.001	-	0.004-0.006	-
N	-	<0.01	<0.02	0.05	0.02-0.04	<0.0005
Si	0.2	0.1	<0.3	<0.1	<0.05	0.1
Ti	-	LAP	LAP	<0.015	<0.02	-
Fe	BAL	BAL	BAL	BAL	BAL	BAL

The steel with the best properties in the USA was ORNL 9Cr-2WVTa steel [53]. Furthermore, in 1992, the Japanese modified F82H and JLF-1 steels formed the basis of a continuing International Energy Agency (IEA) Collaborative Program to evaluate and develop

these RAFM steels for use in fusion reactors [54]. Based on the earlier work on RAFM steels, a new composition called EUROFER-97 was developed in Europe in 1997, which has now replaced the MANET II steel as the reference structural material for the European DEMO breeding blanket concepts [55]. In China, China Low Activation Martensitic steel (CLAM) was designed and developed firstly in Institute of Plasma Physics, Chinese Academy Sciences (ASIPP) in 2002, in the wide cooperation with the institutes and universities in China and oversea [52]. Some efforts were also paid to developing the CLF steel in SWIP in 2007 [56].

1.3.2 Several advanced RAFM steels

1.3.2.1 ORNL 9Cr-WVTa

The earliest low activation steels were proposed mainly at the Oak Ridge National Laboratory (ORNL), Hanford Engineering Development Laboratory (HEDL), and GA Technologies, Inc. (GA) in the 1980s in USA [57].

The original consideration indicated that the Cr-W steels may offer the best possibility as replacements for traditional Cr-Mo steels. W is in the same group of the periodic table and displays similarities to Mo when it is used as an alloying element in steels. This similarity suggested an initial steel composition of 2% W, which is the amount of W required to obtaining an atomic concentration similar to that for 1% Mo. It was also decided to add V in an amount similar to that present in the Cr-Mo steels [57].

Initial studies at Oak Ridge National Laboratory (ORNL) were on steels with 2.25 to 12% Cr [58]. Eight 25 kg electroslag-remelted heats were prepared by Combustion Engineering, Inc., Chattanooga, TN, USA [58]. The results showed, of the original eight ORNL steels studied, the 2.25Cr-2WV steel had the highest strength [59]. However, the impact toughness of 2.25Cr-2WV, as measured with subsize Charpy specimens, was inferior to that of 9Cr-2WVTa steel. The 9Cr-2WVTa had comparable tensile properties and superior Charpy impact properties to 9Cr-1MoVNb and 12Cr-1MoVW. An important property for ferritic steels is the effect of irradiation on impact properties. The 9Cr-1MoVNb and 12Cr-1MoVW steels irradiated to 13 dpa at 400°C in the Experimental Breeder Reactor (EBR-II), and showed that the DBTT increased by about 52 and 124°C, respectively [60]. While, the DBTT only has an increase by 15°C for 9Cr-2WVTa irradiated to 13 dpa in the Fast Flux Test Facility (FFTF) [61]. In the latter experiments, the 2.25Cr-2WV was again inferior, having a shift in DBTT of 145°C.

Thus, the steel with the best properties in USA was proved to be ORNL 9Cr-2WVTa steel.

Work in progress at ORNL has been done to commercialize the steels and developing a database to apply it for an ASME Code Case.

1.3.2.2 F82H

At an International Energy Agency (IEA) sponsored workshop for fusion Ferritic/Martensitic steels in Tokyo in 1992, a proposal was made for an international collaboration on determining the feasibility of using ferritic steels for fusion [54]. The Japanese delegation at the meeting proposed to make available large heats of RAFM steels that could be used in the collaboration between Japan, Europe, and USA.

In subsequent IEA meetings, a modified F82H composition was determined. In 1993 a 5-ton heat of this F82H-IEA (Fe-7.5Cr-2W-0.2V-0.4Ta-0.1C) steel was ordered by the Japan Atomic Energy Research Institute (JAERI) and produced, and processed into 7.5-and 15-mm-thick plates by a contract with NKK Corporation [54]. In1995, a second 5-ton heat was produced by NKK, and processed into 15 and 25-mm-thick plates that were used primarily to make tungsten inert gas (TIG) and electron beam welds [54].

The unirradiated physical and mechanical properties were included in the testing phase for the large heats of F82H and have been almost completed by several years. A computerized database has been developed that is available to the international community [62]. The basic tensile and impact properties are shown in *Figs.1-4* and *1-5*.

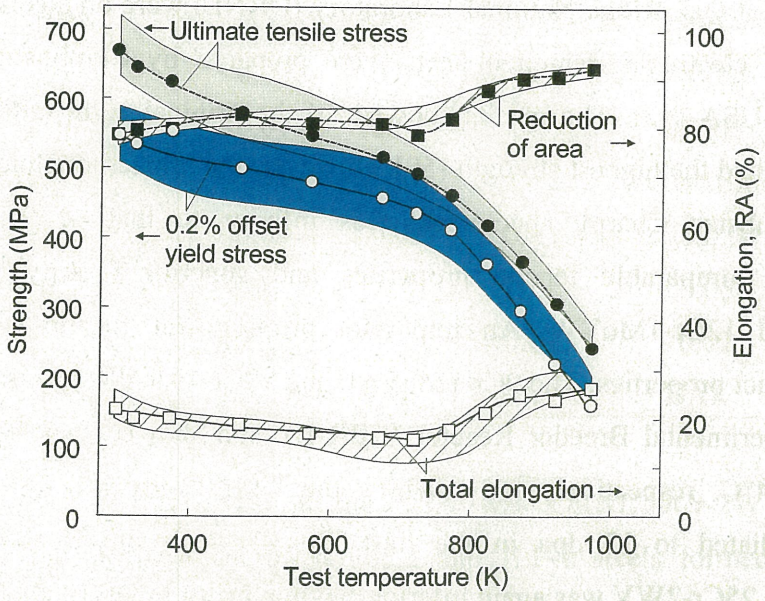

Fig. 1-4 Tensile properties of F82H IEA heat [64]

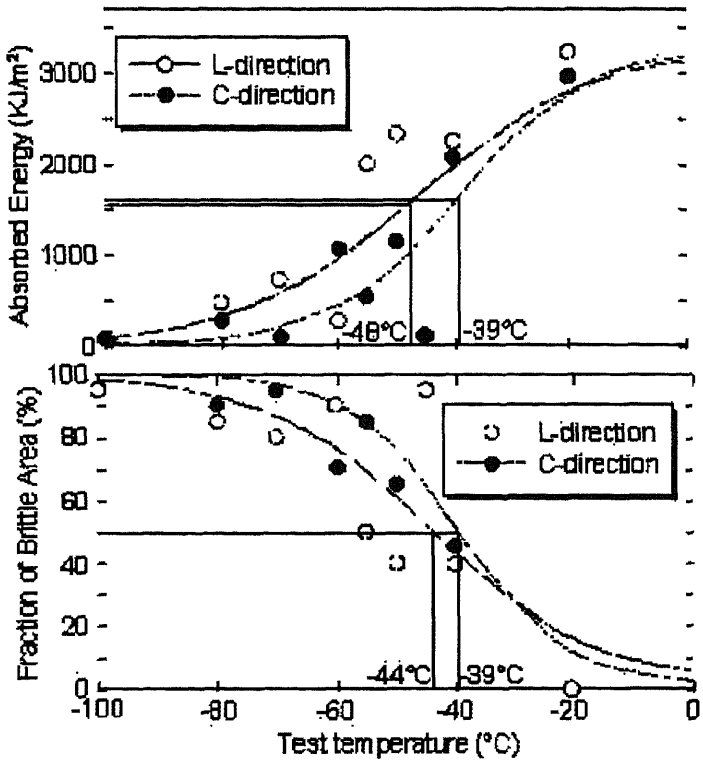

Fig. 1-5 Charpy impact test results of F82H IEA heat [64].

In addition, to determining the irradiation resistance, the F82H steel has been included in over twenty neutron irradiation experiments conducted in the High Flux Isotope Reactor (HFIR) in the USA, in the Japan Research Reactor (JRR-4) and the Japan Materials Test Reactor (JMTR) in Japan, and the High Flux Reactor (HFR) in Netherlands [63]. The results for F82H were in general agreement with results for other experimental 7-9Cr RAFM steels that show improved properties over conventional Cr-Mo steels.

1.3.2.3 JLF-1

As the another steels for IEA test program, JLF series steels have been provided from the Japanese university activity, JUPITER program, which has the basic compositions of Fe-0.1C-XCr-2W-0.2V-0.07Ta-0.05N [65]. The Cr concentration varies from 2.25 to 12 wt% (JLF-1: 9Cr, JLF-3: 7Cr, JLF-4: 2.25Cr, JLF-5: 12Cr). A small amount of titanium (0.015Ti) was added to 9Cr and 12Cr steels (JLF-2 was JLF-1 + Ti, JLF-6 was JLF-5 + Ti) in order to suppress void formation, and also a small amount of nitrogen (0.05%N) was added for high temperature mechanical property improvement. The main purpose is to optimize chemical composition range with a good balance of fracture toughness and creep resistance under irradiation.

The results [65] showed that the DBTT increased only slightly but the creep strength increased significantly with increasing Cr concentration from 2 to 10%, where the steels consisted of the bainite or martensite phase. However, the DBTT increased abruptly and the creep strength decreased at Cr concentrations above 10%, where the δ-ferrite grains formed. These results suggest that the optimum concentration of Cr is located at 7-10%. Moreover, the 7-9 Cr% steel have a good resistance to irradiation embrittlement [66], as shown in *Fig. 1-6.*

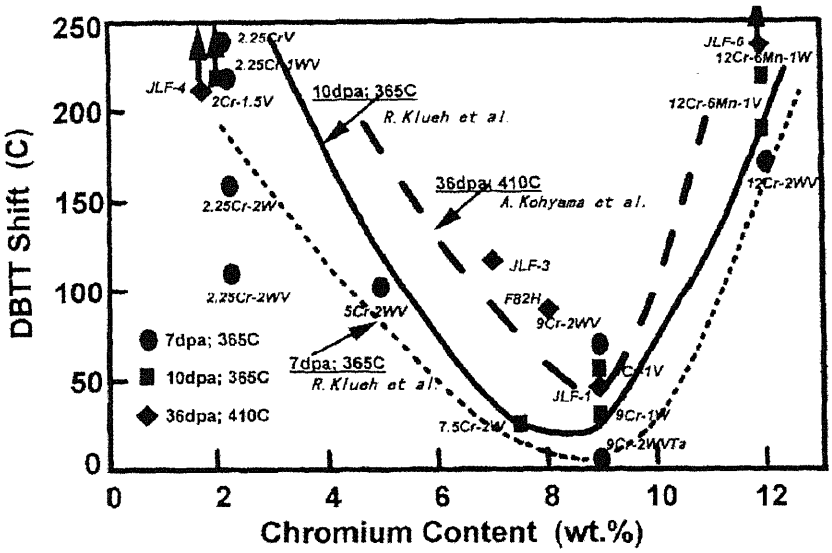

Fig.1-6 Effects of Cr content on DBTT shift for low activation ferritic steels by neutron irradiation in FFTF [66].

JLF-1 presented excellent tensile and creep properties, and resistance to neutron exposure up to 60 dpa in FFTF between the irradiation temperatures of 365 and 600°C [65]. This was encouraging to move to the next step to make large heats for large scale material tests for DEMO.

Thus, the first 1-ton heat of JLF-1 was produced in 1995 with the 7-mm- and 15-mm-thickness plates [54]. This heat was mainly used to obtain the basic mechanical properties and neutron and charged particle irradiation experiments including HFIR irradiation.

The second 1.5-ton large heat of JLF-1 was produced in 1996 and processed into the plates with a thickness of 15 and 25 mm [54]. The emphasis was to investigate the joining technology, performance of welded joints and fracture toughness.

The basic properties and some preliminary data on irradiation effects and microstructural stability obtained so far are quite promising for JLF-1 to application in fusion reactors.

Recently, several new 200-kg ingots of JLF-1 were produced with the small addition of N content, called as JLF-1 (JOYO-II-HEAT). These ingots were forged and rolled into the plates

with the thickness of 25 mm. Some research work has being carried out in the collaboration with NIFS and other universities [67, 68].

1.3.2.4 EUROFER 97

As a conclusion of a development carried out in several EU associations, an alloy designated EUROFER 97 was developed [55]. On the basis of far-reaching experience of precursor OPTIFER steel, the contents of Cr, Ta, and W were specified carefully for EUROFER 97. Since the DBTT in impact tests reaches a minimum at 9% Cr, and in order to achieve a better corrosion resistance, 9% Cr was regarded to be appropriate. Ta stabilizes the grain size by carbide formation and improves DBTT and strength. About 1% W represents a good compromise regarding low activation, DBTT, tensile strength and ductility, creep strength, and also has a higher tritium breeding ratio (TBR). To achieve reduced activation behavior, the radiological undesired elements, such as Nb, Mo, Ni, Cu, Al and others, have to be limited to the wppm level.

An industrial batch of 3.5 ton was specified and produced in 1997 with the presently available steel manufacturing technology [55]. Different semi-finished products (bars, plates and tubes) with a sufficiently low content of radiologically unwanted impurities like Nb, Mo and Ni were delivered. A characterization program has been undertaken to determine the relevant mechanical and physical-metallurgical properties in order to qualify EUROFER for fusion application. Presently, the material is extensively tested in different European laboratories.

The research results showed that the EUROFER 97 can be manufactured in industrial scale with reproducible properties. First results of the characterization campaign are also promising. The mechanical and compatibility properties are adequate. Fig.*1-7* shows the creep property results, which is comparable to F82H [69].

In order to achieve lower contents of undesirable elements, a further reduction into the sub-ppm-range is necessary on the way from reduced to real low activation alloys. A new EUROFER 97/2 batch with identical specification of alloying elements and further reduced impurities has to be ordered to check the reproducibility of steel making, improve the production of semi-finished components and provide additional material for further technology tests [55].

Regarding to increase the upper operating temperature, the improved oxide dispersion strengthening steel called EUROFER-ODS was produced by alloying the fine Y_2O_3 and studied in laboratory scale [70]. Chemical optimization, such as the C, Ti and Cr, is necessary to retain a martensitic structure. Also, a broadening and improvement of fabrication processes for the

production by powder metallurgy, mechanical alloying, hipping, extrusion techniques, welding and optimization of final thermo-mechanical treatments are of great importance.

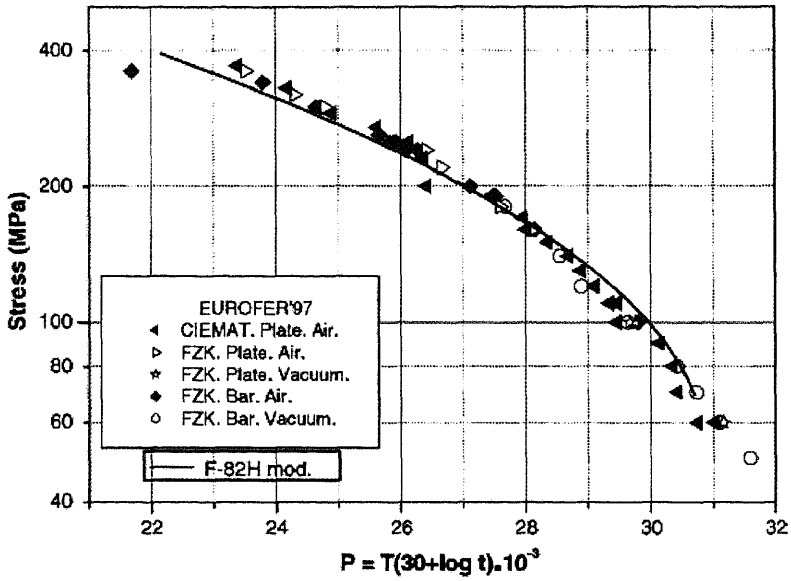

Fig.1-7 Larson-Miller parameter of the EUROFER 97 steel and the F82H-mod steel in the as-received condition [69].

1.3.2.5 CLAM

Recent several years ago, based on the excellent experiences of other RAFM steels development in the world, the China Low Activation Martensitic (CLAM) steel was designed and produced in China [52, 71]. The composition of CLAM steel has been adjusted to balance the performance, such as changing the typical content of W from 2.0 to 1.5% to decrease the amount of Laves phase possibly precipitated. Ta content was increased to 0.15% with the purpose to produce smaller prior-austenite grain and higher density of spherical Ta-rich precipitates (TaC), and thus to increase the tensile strength and long-term creep resistance. Addition of a suitable amount of Mn is with the aim to improve the compatibility with liquid metal.

A lot of work has been carried out in the wide collaboration between the institutes and universities in domestic and overseas [67, 71-74]. Several 5 and 25 kg ingots of CLAM steel were prepared by a vacuum induction melting furnace with highly purified raw materials from 2003 to 2005. In 2006, several large ingots of 300 kg were produced and then forged and rolled into plates with 10, 15 and 20 mm thickness. In addition, other research work were also carried out widely, including optimization of fabrication techniques, characterization of physical and mechanical

properties before and after irradiation, evaluation of compatibility with liquid metal, and development of the criteria for fusion material designs.

Fig.*1-8* shows the results of electron-beam irradiation on swelling for CLAM steel. CLAM exhibits a good resistance to swelling at test temperature, where the peak swelling was determined to be about 0.3% for a damage level of 13.8 dpa. [74].

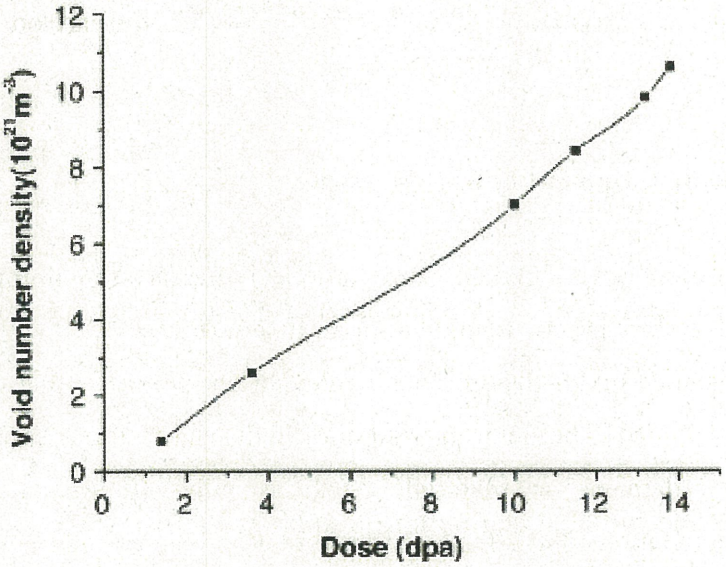

Fig.1-8 Dose dependence of void number density up to 13.8 dpa for irradiation at 723 K for CLAM steel [74].

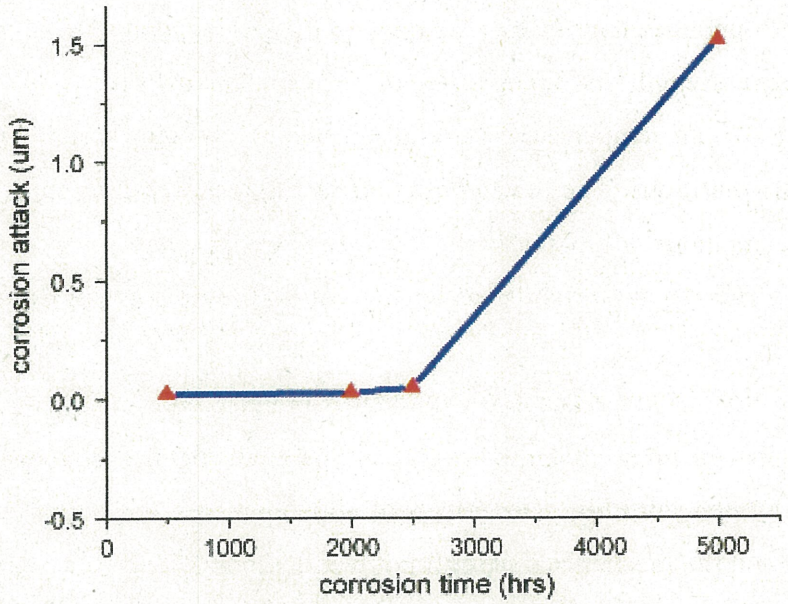

Fig.1-9 Metal weight loss vs. exposure time for CLAM in flowing LiPb loop [72].

Fig.1-9 showed the compatibility results of CLAM steel with flowing liquid LiPb, which was performed at 480°C for 5000 h with a flow rate of 0.08 m/s in DRAGON-I loop [72]. After 2500 h, the corrosive attack began to occur partially because of the loss of passivated oxide layers. In addition, the elements such as Fe and Cr were dissolved into the LiPb.

According to all the results up to date, CLAM has good tensile, creep, and irradiation properties, and most of them are comparable to those of the other RAFM steels. The optimization of chemical compositions and production of large ingots (about > 1 ton) are ongoing.

1.3.3 Critical issues for development of RAFM steels

Although great progress was achieved, some critical issues are remaining and necessary to resolve for RAFM steels before practical application in fusion reactors.

(1) Irradiation resistance under fusion reactor relevant conditions is one of the major issues for structural materials [75-76]. The neutron irradiation will lead to the present of transmutation product He and heavy damage on materials, such as microstructure instability and thus mechanical property degradation. The effects of transmutation element of He on deformation and fracture mechanism is still not clear. For full understanding of the irradiation effects, two approaches are being investigated: (a) modeling of irradiation damage and irradiation effects, and (b) construction of the International Fusion Materials Irradiation Facility (IFMIF) to produce an intense source of 14 MeV neutrons [77].

(2) The upper operation temperature window is limited to about 550°C for RAFM steels by the decrease in yield strength and creep strength [75-76]. The efforts should be paid to increase the creep strength at high temperature, such as further optimization the chemical compositions and heat treatment conditions. The development of ODS steels with excellent creep property are one of promising methods to increase the operation temperature [70]. However, fabrication techniques of ODS are not yet established to the required level and the present experiences are still very limited.

(3) Compatibility of RAFM steels with liquid breeder and coolant is an uncertain issue [28-30]. A number of different coolants have been proposed for fusion reactors, including water, LiPb, Li, He, and molten salt Flibe. The effects of alloy elements and impurities on corrosion rate and mass transfer, and the mechanism are still not well understood.

(4) Possible adverse effects of RAFM steels on plasma control and performance because of the ferromagnetic properties is still an issue [75].

1.4 Status of the thermal ageing on RAFM steels

1.4.1 Definition of thermal ageing and possible effects

Generally, ageing is one of heat treatment processes, accompanied by a forming of a finely dispersed particle of second phase within the original material phase matrix [78]. These precipitants are effective barrier to impede dislocation motion and leading to substantial hardening of material. If the ageing process is continued so long that the precipitants are coarsen, the precipitates are less effective as dislocation barriers. This effect is called overageing. The overageing also can lead to the change in other microstructure.

Thermal ageing of materials used in fusion reactors is a time and temperature dependent degradation mechanism, which may results in a change of mechanical property and recovery of microstructure [79-80]. The structural materials of DEMO and future fusion power systems are required to be used for more than 10 years. Therefore, the long-term and elevated-temperature thermal ageing is an important criterion and concern for blanket design with RAFM steels.

In high stress and low temperature design region, decrease in the yield stress and resulting softening by ageing can reduce the maximum operation temperature. The effect of thermal ageing on tensile property is schematically shown in *Fig.1-10*.

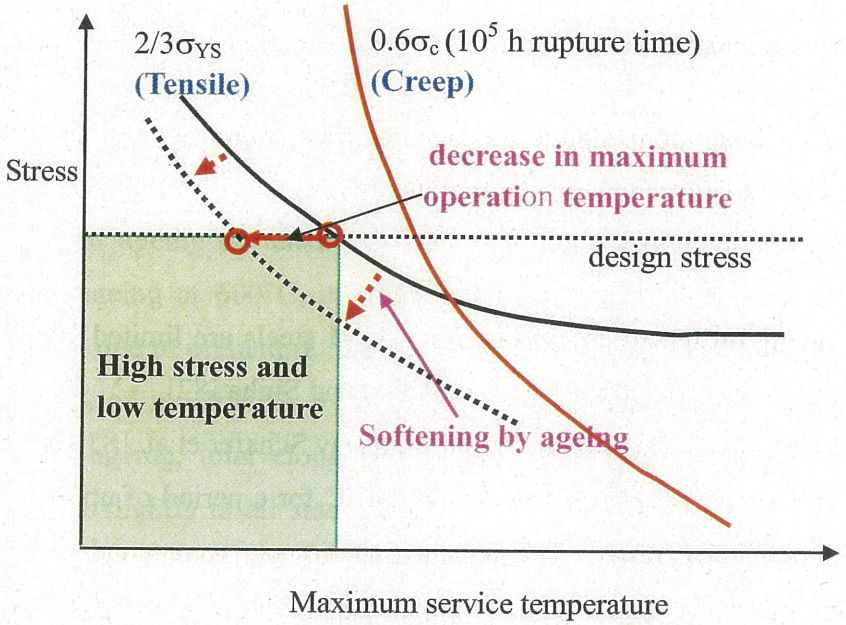

Fig. 1-10 Possible softening of tensile stress by thermal ageing

In low stress and high temperature design region, the design stress is governed mainly by creep rupture stress. The ageing may affect the creep property, and thus influence strongly the maximum operation temperature, as schematically shown in *Fig.1-11*.

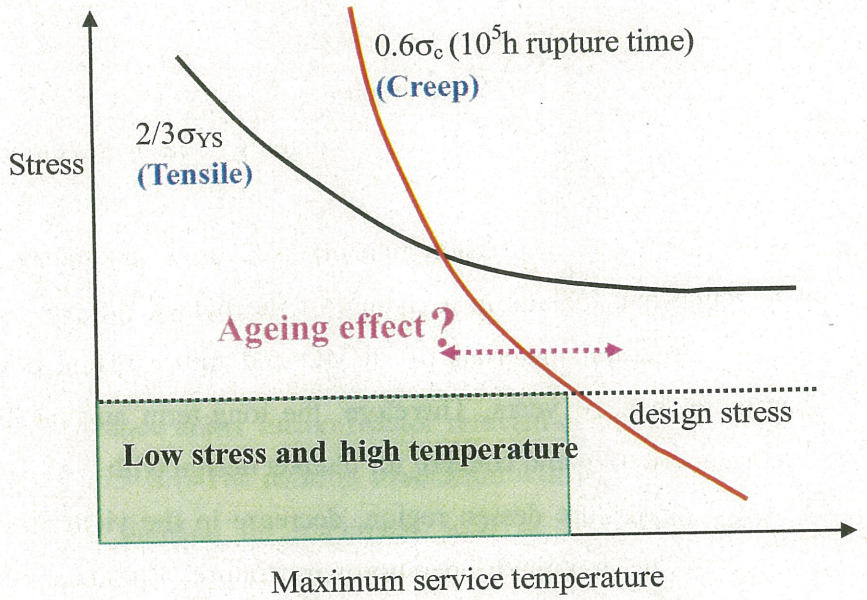

Fig. 1-11 Possible effect of thermal ageing on creep property for RAFM steels

1.4.2 Previous study on ageing effects for RAFMs

Some studies have been done about the ageing effects on the mechanical property and microstructure for RAFM steels, which are summarized below:

(1) Tensile properties

The effects of ageing on tensile properties for RAFM steels are limited when temperature is lower than ~800 K, which was concluded by Alamo [81] and Shiba [82].

Ageing on OPTIFER series steels was studied firstly by Schafer et al. [83]. The materials were subjected to ageing experiments between 550°C and 650°C for a period of up to 10000 h and then the mechanical properties were tested. The tensile experiments were conducted at 250°C. The results of tensile properties before and after ageing are shown in *Fig. 1-12*.

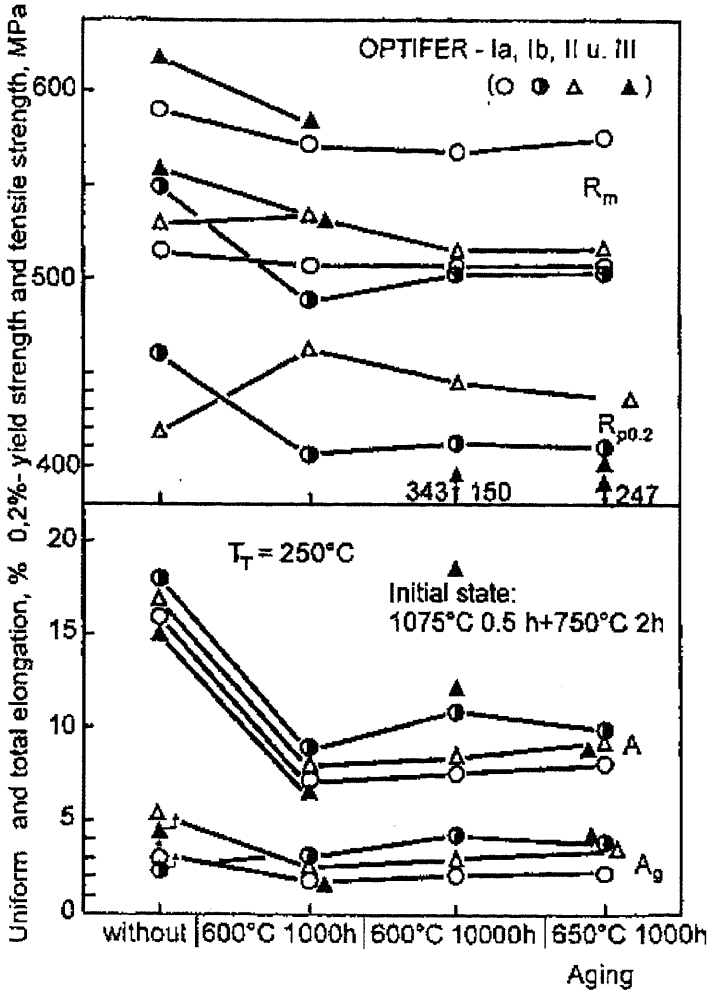

Fig. 1-12 Tensile properties at 250°C of the steels OPTIFER-Ia, Ib, II and III after ageing [83]. The OPTFER steels have a basic compositions of 9Cr-0.1C-0.25V-0.5Mn with different contents of W and Ta (Ia: 1%W + 0.066%Ta, Ib:1%W+0.163%Ta, II:0.018%Ta, and III:1.6%Ta). R_m: ultimate tensile strength, $R_{p0.2}$: yield strength, A: total elongation and A_g: uniform elongation).

The influence of ageing on tensile strength was very strong for OPTIFER III. After a few thousand hours of ageing at 600°C, strength of OPTIFER III decreased rapidly, similar to the hardness, which was due to premature recrystallization or grain coarsening. The steel OPTIFER Ib only lost about 10% of its strength by ageing. The steels OPTIFER Ia and II remained nearly unchanged. Due to ageing, total elongation of all OPTIFER steels droped markedly. Uniform elongation decreased slightly in all steels (except for OPTIFER Ib). Ultimate tensile strength and yield strength of the steel OPTIFER-IV decreased by about 15 and 20 MPa, respectively, whereas total and uniform elongation remained roughly unchanged. The total elongation dropped slightly or considerably for OPTIFER, which was indicated to dependent on the prior heat treatment conditions.

Some work about ageing effect on F82H-IEA steel was done by Shiba [82]. Thermal ageing experiments were carried out at 450, 500, 550 and 600°C for 1000, 10000, 30000 h. The results showed that the ageing did not have much effect on tensile properties when temperature was lower than 600°C.

The JLF-1 steel was aged at temperature relevant to fusion applications (250-550°C) up to13500 h [79]. The tensile results showed that the steel displayed very stable strength values, as showed in *Fig.1-13*, and just a slight decrease of the reduction in area was detected especially after ageing at 550°C.

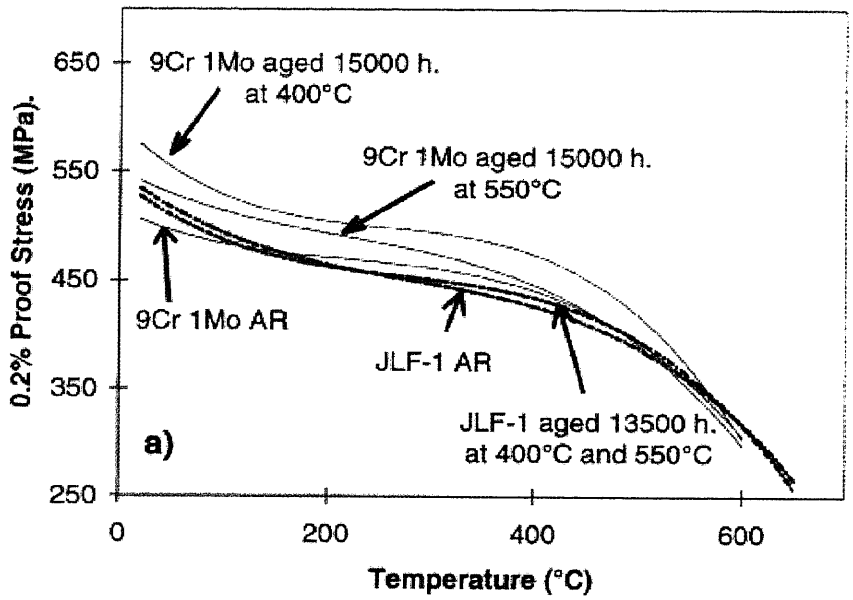

Fig.1-13 Evolution of the 0.2% proof stress (yield stress) with ageing of JLF-1 at normalization and tempering (N&T) initial conditions compared with other steels [79].

A series of ageing work has been done for EUROFER 97. After ageing at 550°C for 5000 h and 600°C for 1000 h, no degradation of tensile properties (ultimate tensile strength and yield strength) was detected, compared with the as-received state, as shown in *Fig.1-14* [84]. The microstructural stability can be considered as the main reasons for small influence of ageing on tensile properties.

The research by Lindau [85] also showed that ageing at 580 and 600°C up to 3300 h caused only a marginal decrease in the tensile strength.

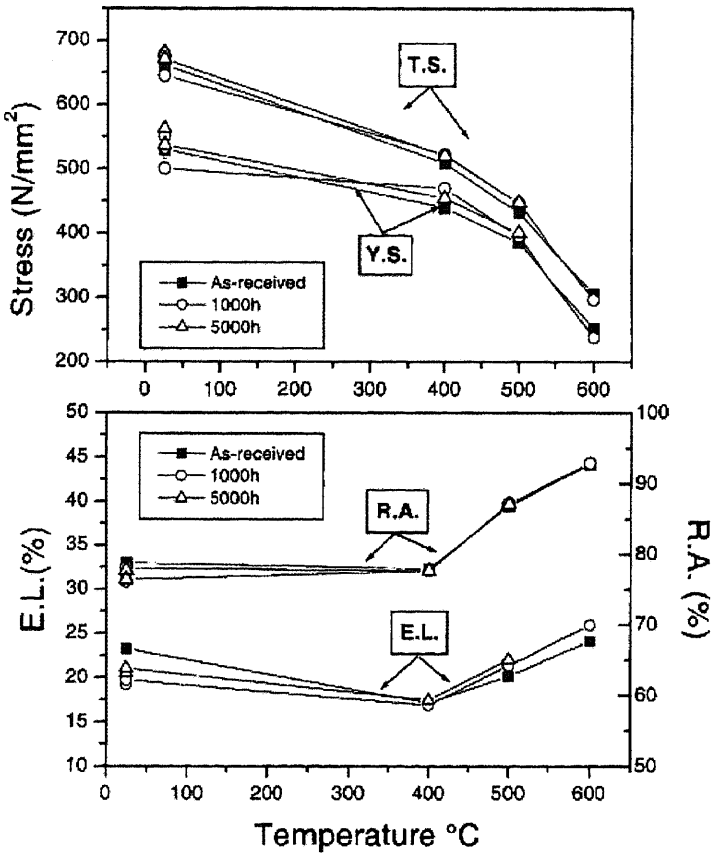

Fig. 1-14 Tensile properties of the EUROFER 97 steel in the as-received condition and after ageing at 400 and 500°C [84].

(2) Impact properties

Most of work about the effects of thermal ageing was focused on the impact property. The long-term thermal ageing may lead to the significant upward shift of DBTT for RAFM steels, because of the formation of brittle Laves and other phases, the coarseness in grain size, and possible other phases.

The research by Schafer [83] showed that F82H-mod steel exhibited a remarkable increase in DBTT due to aging, as shown in *Fig.1-15*. The DBTT increased about 9 K after ageing at 550°C for 5000 h, 27 K at 600°C for 5000 h, 68 K at 600°C for 10000 h, and 20 K at 650°C for 1000 h (without figure), respectively.

Shiba [82] reported the results after thermal ageing up to 10000 h for F82H-IEA, as shown in *Fig. 1-16*. The impact toughness for F82H decreased considerably, with the increase in DBTT at the ageing temperatures above 800 K, in agreement with the finding of Schaefer [83].

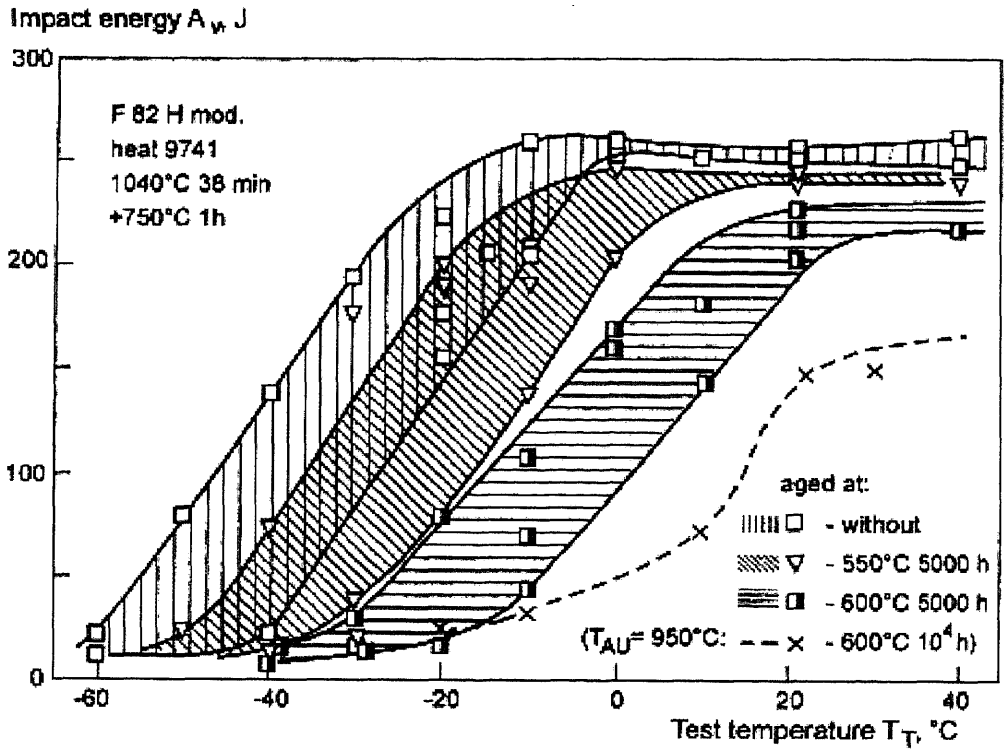

Fig. 1-15 Impact energy of the F82H-mod steel as a function of the test temperature showing an increase in DBTT (up to +68 K) after ageing [83].

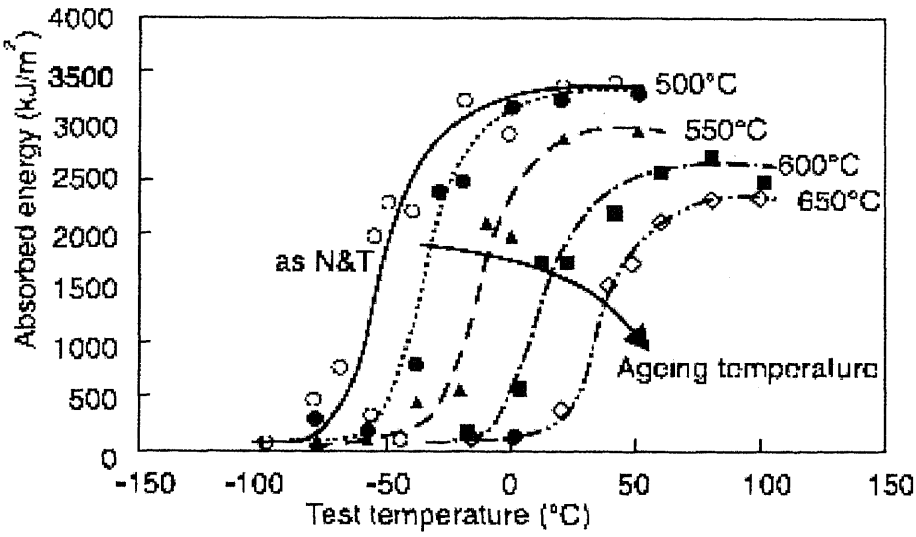

Fig. 1-16 Absorbed impact energy of F82H after ageing for 10000 h at indicated temperatures [82]

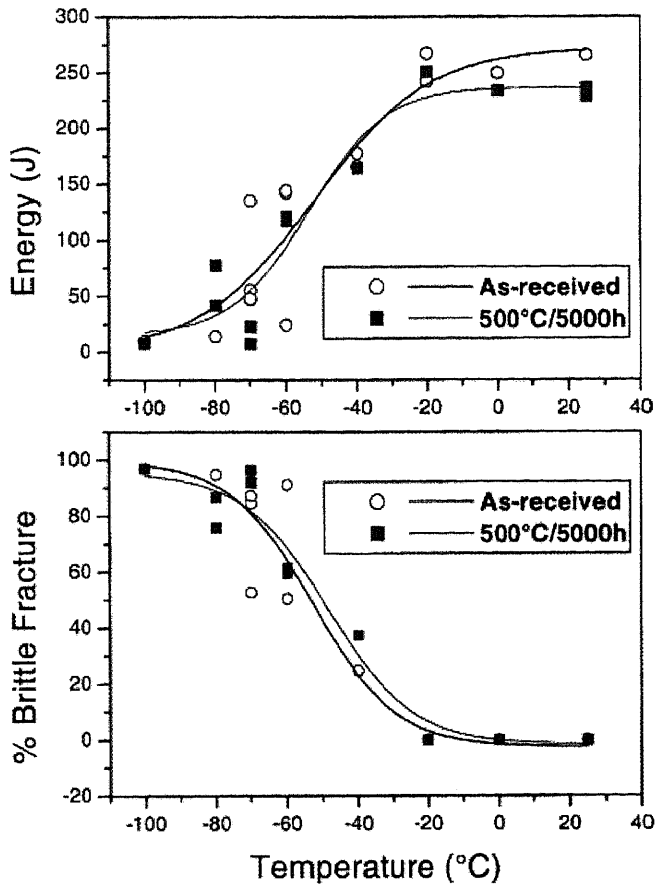

Fig. 1-17 Impact curves for the EUROFER 97 steel in the as-received condition and after ageing at 500°C for 5000 h [84].

EUROFER 97 has a better impact property after thermal ageing [84]. As shown in *Fig.1-17*, the DBTT stayed constant and the USE decreased approximately 30 J after ageing.

The EUROFER 97 exhibits a better toughness after ageing than other RAFM steels, like F82H-mod. The lower DBTT is basically attributable to the finer prior austenite grain size of the EUROFER 97, mostly due to the higher Ta (0.10%) and V (0.19%) concentration compared with F82H-mod (0.005%Ta and 0.14%V).

(3) Low cycle fatigue properties

Thermal ageing will affect the fatigue properties. Fernandez et al. [76] have performed some low-cycle fatigue tests on F82H aged for 5000 h. The results showed an increase in fatigue strength after ageing in unnegligible content. However, the data is limited.

(4) Creep properties

RAFM steels will be long-term loaded at higher temperature for application in fusion reactors. Thus the creep behavior is very important. However, during the long-term creep experiments, the ageing effect may also operate. It is not easy to separate the ageing effects and creep effects.

Some work on EUROFER 97 was done. The creep specimens of EUROFER 97 were first aged at 580°C for 3000 h and 600°C for 1050 h, then tested in the creep facility at 550°C for 10000 h [86]. The results showed that an ageing effect cannot be practically detected.

Tamura reported some results of ageing effects on creep rupture time for pre-F82H IEA steel [87]. As shown in *Fig. 1-18*, after aging at 600°C for 30 000 h, the rupture time was shorter at higher stresses than that of normalized and tempered condition. However, at lower stresses the difference between the aged and the unaged material became smaller. On the other hand, ageing at 650°C for 30 000 h caused a significant decrease in the rupture time.

However, studies on the ageing effects on creep property for other RAFM are still very limited.

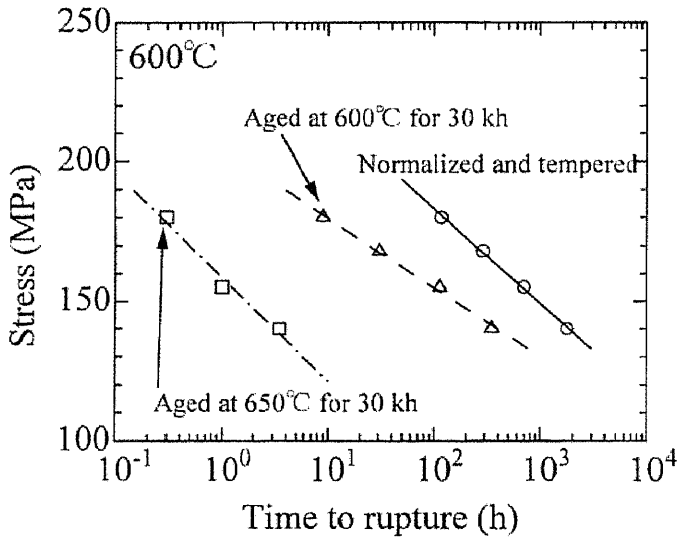

Fig. 1-18 Stress vs. time to rupture diagram for pre-F82H IEA steel

(5) Microstructural evolution

Many researches showed that no significant change in microstructure can be detected after thermal ageing at temperature lower than 500°C for short time [79-80, 85, 88]. However, during the long-term ageing, the microstructure will change, such as the coarseness of precipitates $M_{23}C_6$, formation of Laves phase and M_6C, and recovery of sub-microstructure.

It was found by Shiba et al., the Laves phase formed after ageing at 600°C for 30 000h for F82H steel, as shown in *Fig. 1-19* [88]. The effects of thermal ageing on precipitates are also shown in the Temperature-Time-Precipitates (TTP) diagram curves, *Fig.1-20* [88]. It shows that the M_6C will appear at 500 and 550°C, and the Laves phase appear over 600°C after ageing for ~10000 h, which is less than the expected ITER-TBM life time. Thus the formation of M_6C and Laves is already the issue for the TBM.

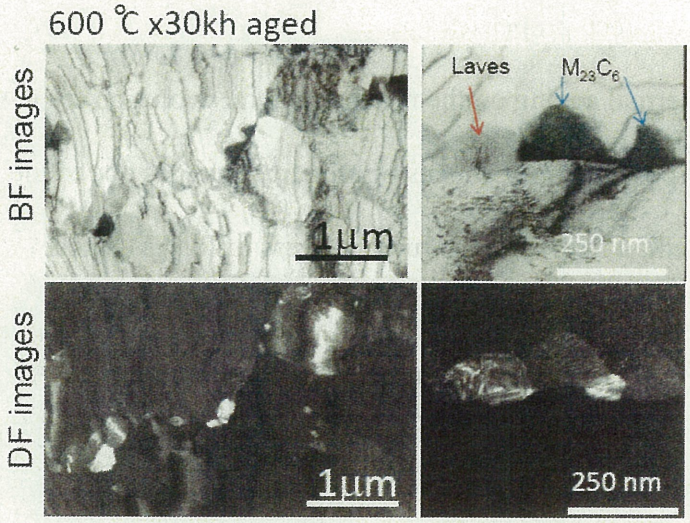

Fig.1-19 Large Laves phase is formed adjacent to $M_{23}C_6$ for F82H steel after ageing at 600°C for 30 000 h [88].

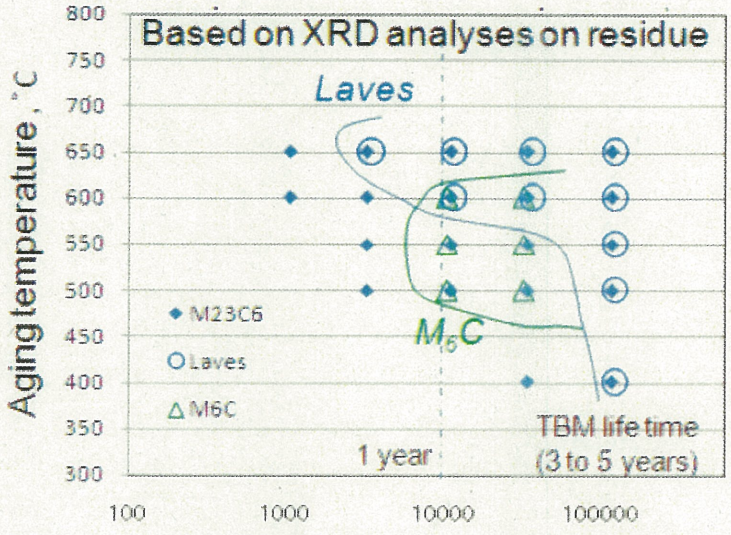

Fig.1-20 The Temperature - Time - Precipitates curves for F82H steel [88].

1.5 The objectives of this work

The purposes of the present study are:

1) To examine the effects of thermal ageing on the mechanical properties for RAFM steels with respect to

- Hardness
- Tensile properties
- Creep properties

2) To examine the thermal ageing on the microstructural evolution for RAFM steels.

3) To investigate the possible mechanisms of property changes due to thermal ageing.

4) To develop the method to predict the rupture stress of RAFM steels in the typical designed life of fusion blanket including ageing effects.

5) Discussion on critical issues and emphasis in the development of RAFM steels.

CHAPTER 2

Experimental Procedure

2.1 The preparation of materials

The JLF-1(JOYO-II-HEAT) was melted into a 200 kg ingot in vacuum and then was fabricated into a 25-mm-thick plate. The CLAM (0603 HEAT) was melted in a vacuum induction furnace to an ingot of 300 kg by high pure raw materials, and followed by hot-forging and rolling into a 15-mm-thick plate. The preparation process for CLAM steel is described in *Fig. 2-1*.

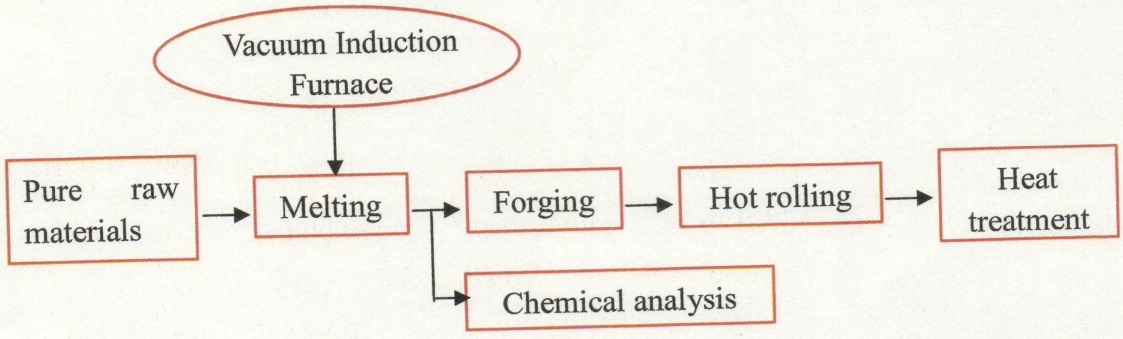

Fig. 2-1 Flow chart for the preparation of CLAM steel

2.2 The chemical compositions and heat treatments

The chemical compositions of JLF-1 (JOYO-II-HEAT) and CLAM (0603 HEAT) steels are listed in *Table 2-1*, and the heat treatments conditions are listed in *Table 2-2*.

Table 2-1 Chemical compositions of JLF-1(JOYO-II-HEAT) and CLAM (0603 HEAT) (in weight%)

	Cr	W	C	Mn	V	Ta	O	N	P	S	Fe
JLF-1	9.00	1.98	0.09	0.49	0.20	0.083	0.0019	0.0150	<0.003	0.0005	Bal.
CLAM	8.94	1.45	0.13	0.44	0.19	0.15	0.0017	0.00585	0.0027	0.004	Bal.

Table 2-2 Heat treatment conditions for (JOYO-II-HEAT) and CLAM (0603 HEAT) steels

Type of steel	Normalization	Tempering
JLF-1	1323 K / 60 min / air cool	1053 K / 60 min / air cool
CLAM	1253 K / 30 min / air cool	1033 K / 90 min / air cool

2.3 The ageing experiments

Because of the limit of irradiation volume, the standard specimen is not suitable for the irradiation tests. Therefore, the small specimen testing technology has been developed and applied widely in the fission and fusion reactors field. In this study, the small specimens will be applied as the un-irradiated data for comparison with the irradiation data.

SS-J is a kind of small specimens for tensile tests developed in Japan, which has a gauge section of 5 x 1.2 x 0.25 mm^3. The dimension is shown in *Fig.2-2*. In this work, SS-J specimens were used for ageing experiments and subsequent mechanical property tests.

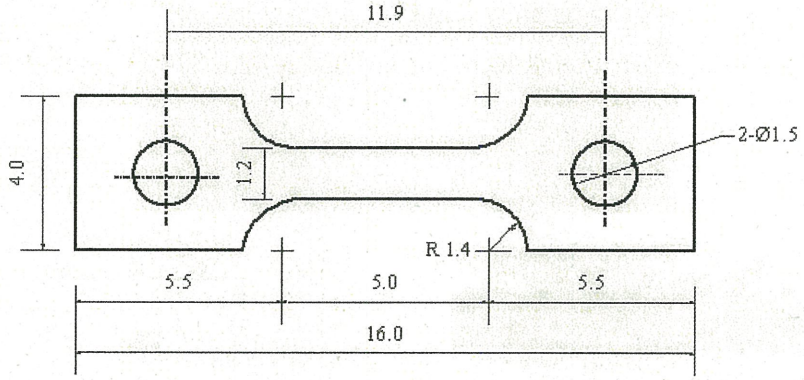

Fig. 2-2 SS-J specimens

The procedure for the sample preparation is described as followed:

At first, the steel plates were cut into small parts and then sliced into thin plates with a thickness of about 0.4 mm. After that, SS-J samples were prepared by using a punching machine. The gauge section of the sample is parallel to the rolling direction. These procedures are shown in *Fig.2-3*.

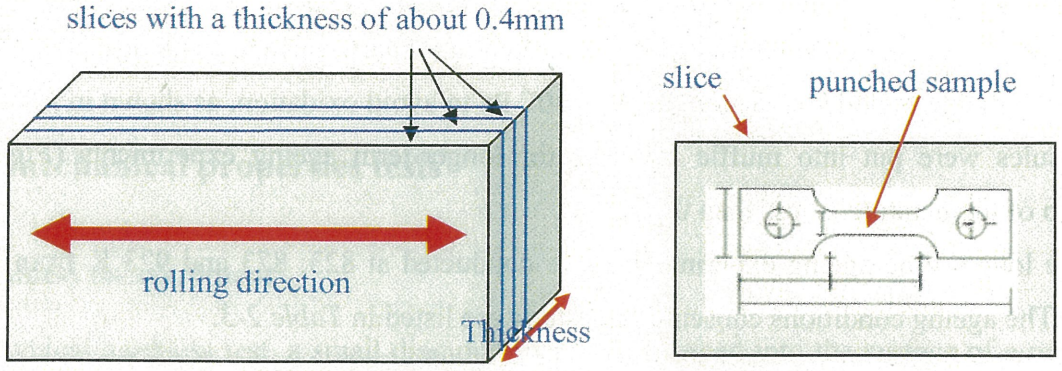

Fig.2-3 Preparation process for samples: sliced and punched

After grinded roughly and cleaned by acetone, the samples were submitted to the ageing treatments. The ageing temperatures were chosen from 823 to 973 K up to 2000 h. The ageing temperatures of 823 and 873 K were to simulate the maximum service temperature, while 923 and 973 K were to accelerate the thermal processes.

Thermal ageing experiments were carried out in two different devices according to the ageing time:

(1) Short-term ageing experiments (≤ 100 h)

The samples were sealed by Zr foils to avoid oxidation and then putted into the infrared image furnace. The furnace has a high vacuum of ~1 x 10^{-4} Pa and accurate control the temperature with an error less than 0.1 K. The device is shown in *Fig.2-4*.

The short-time ageing experiments were carried out at 823, 873, 923 and 973 K in this furnace.

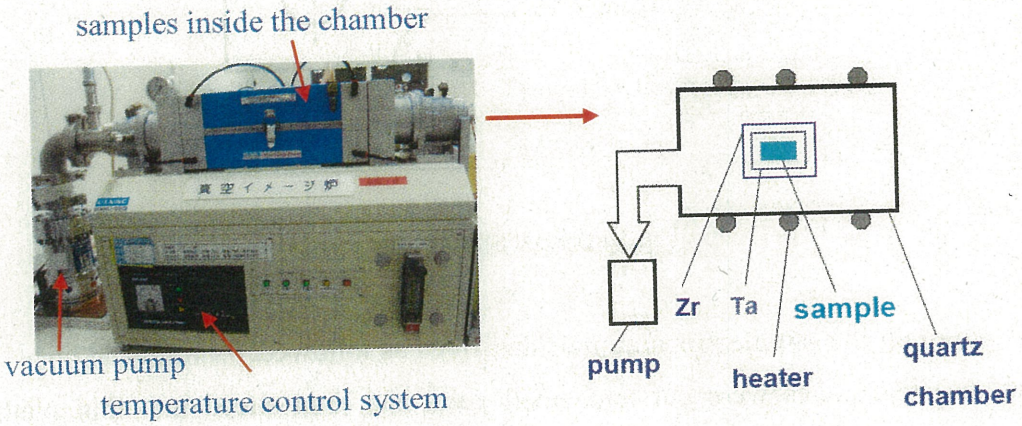

Fig. 2-4 Infrared image furnace for short time ageing experiments

(2) Longer-term ageing experiments for (> 100 h)

The samples were covered by Zr foil and sealed into quartz capsules with about 120 mm length and 15 mm diameter under a vacuum of ~1 x 10^{-4} Pa to avoid oxidation, as shown in *Fig.2-5*. Then, the capsules were put into muffle furnaces for longer-term ageing experiments (*Fig.2-6*). The precision of temperature is less than 0.1 K.

The longer-time ageing experiments were conducted at 823, 873 and 923 K from 500 up to 2000 h. The ageing conditions chosen in this study are listed in *Table 2-3*.

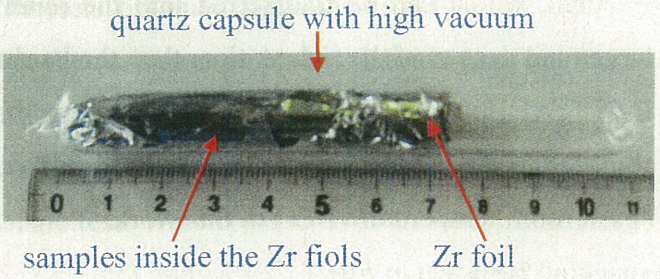

Fig. 2-5 Samples were sealed in quartz capsule under high vacuum

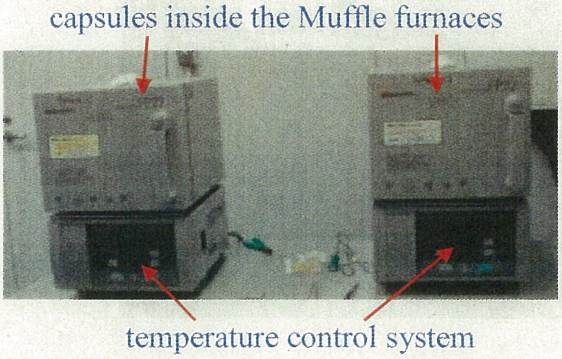

Fig. 2-6 Capsules were inside in Muffle furnaces for long time ageing experiments

Table 2-3 The selected ageing conditions and subsequent tests for JLF-1 and CLAM steels

Ageing time, hr	Ageing temperature, K			
	823	873	923	973
100	○▲ ▮	○▲ ▮	○▲ ▮	○▲◆■▮
500			○▲◆	
1000		○▲◆	○▲◆	
2000	○▲◆■▮	○▲◆■▮	○▲◆■▮	

○: ageing, ▲: hardness measurement, ◆: tensile tests, ■: creep tests, ▮: microstructure analysis

2.4 The mechanical properties tests

2.4.1 Hardness measurement

In a typical hardness test, a small diamond indenter is forced into the surface of a material to be tested, under controlled conditions of load and rate of application. The depth or size of the

resulting indentation is measured, which can be transferred into the relative hardness value. The softer of the material, the larger and deeper of the indentation, then the hardness value is the lower.

After mechanical grinded and electro-polished to about 0.25 mm thickness, the samples of JLF-1 and CLAM were submitted to the hardness tests. Vickers hardness was measured with a load of 300 g and duration of 30 s at room temperature (RT) in this work.

The hardness testing machine is shown in *Fig. 2-7*.

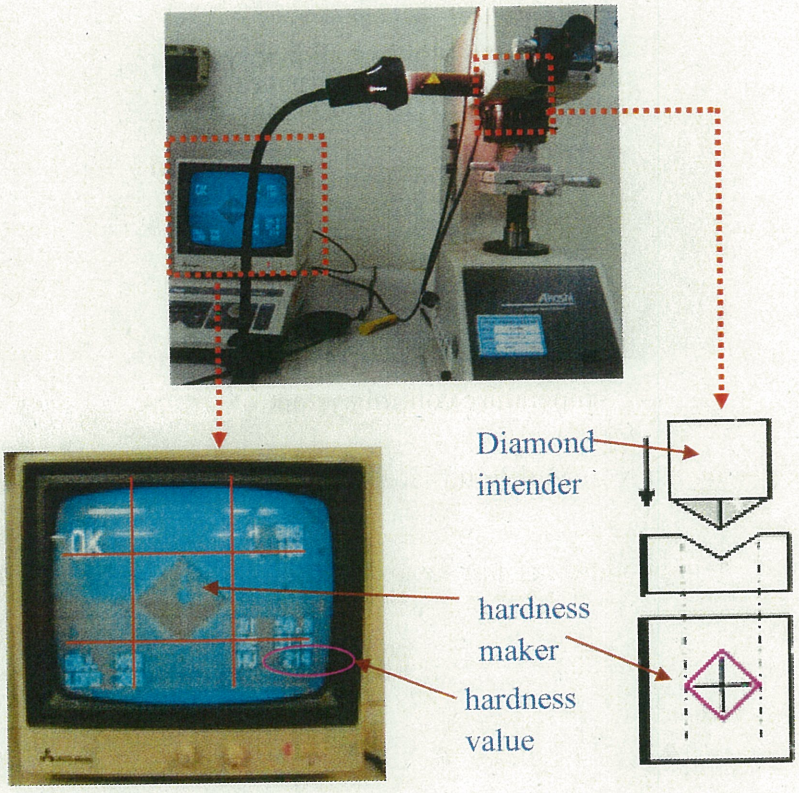

Fig. 2-7 Vickers hardness test machine

2.4.2 Tensile property tests

Tensile test is one of most common mechanical stress-strain tests, which can be used to ascertain several parameters of materials that are important in design [89]. The typical curve for RAFM steels is schematically shown in Fig. 2-8.

The first region of tensile curve is an elastic deformation region. During this region, the stress and strain are proportional to each other. This linear relationship is called Hooke' Law. When the material continues to be deformed beyond this point, the stress is no longer proportional to strain, and permanent, or plastic deformation occurs. After necking, the material will be ruptured finally.

The important parameters obtained from the stress-strain curves include: (1) Yield Strength (point A), σ_{YS}, to measure the resistance to plastic deformation; (2) Ultimate Tensile Strength (point B), σ_{UTS}, to indicate the maximum load that a material can bear; and (3) Total Elongation (point D), TE%, to describe the ductility of a material.

In this work, the tensile tests were conducted at an initial strain rate of 0.2mm/min and the test temperatures of RT, 673, 773, 823 and 873 K. The test at RT was conducted in air, while the tests at the elevated temperatures were in a vacuum of 10^{-4} Pa.

The exterior view of tensile testing machine is shown in *Fig. 2-9*, and the interior view is similar to the creep testing machine, which will be shown later.

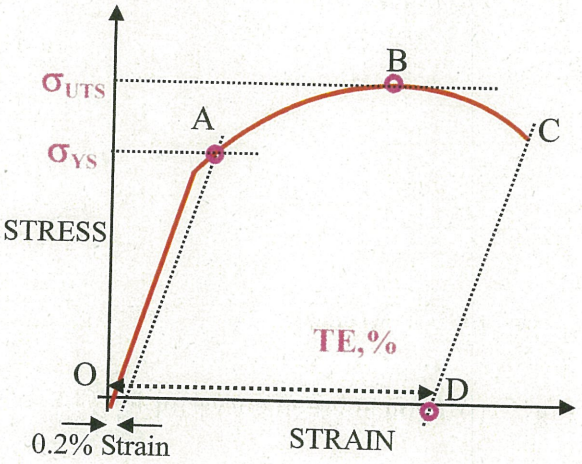

Fig. 2-8 Schematic illustration of the typical tensile curve for RAFM steels

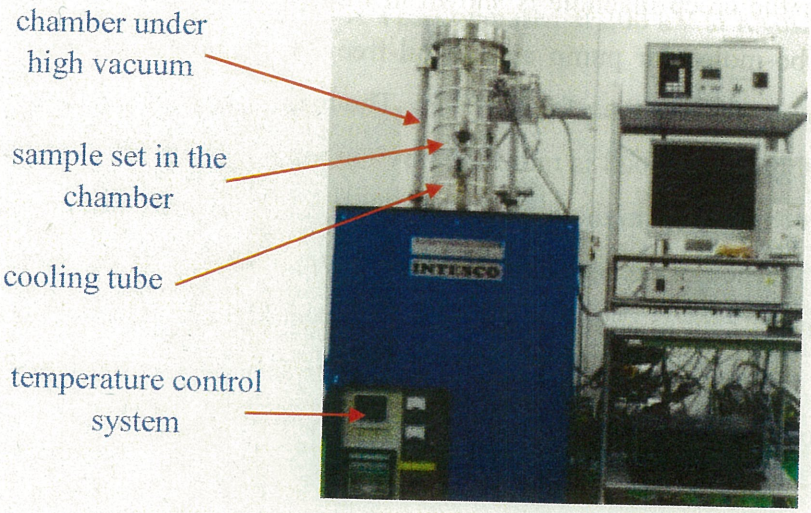

Fig. 2-9 The tensile property test machine

2.4.3 Creep property tests

Creep is defined as time-dependent deformation under constant stress less than yield stress. Usually, creep deformation occurs at elevated temperatures, often greater than roughly 0.5 T_m, where T_m is the absolute melting point of the material.

The typical creep curve of RAFM steels, as shown in *Fig. 2-10*, exhibits three distinct regions: primary, secondary and tertiary. From the secondary stage, the steady-state stage, the minimum creep rate can be obtained, which is the slope of this linear part. In addition, from the point of sample ruptured, the rupture time can be measured.

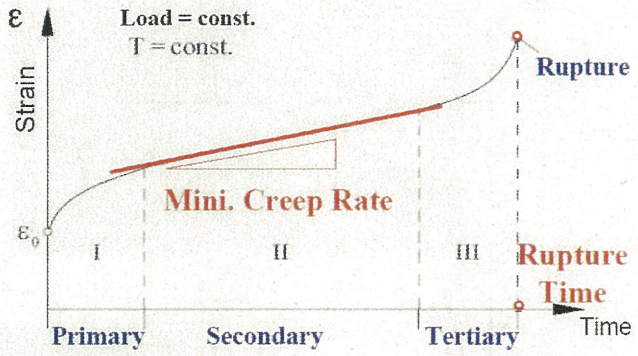

Fig. 2-10 Typical creep curve for RAFM steels

In this work, the uniaxial creep property was tested. The samples for creep tests were the same as those for the tensile tests. The creep temperatures were from 823 to 973 K and the applied stresses were in the range of about 100 to 300 MPa.

The view of the creep machine is shown in *Fig.2-11*. The vacuum system of creep machine consists of a turbo-molecular pump and an oil-free scroll pump, and is sealed by copper metal gasket. The vacuum was less than 1.0×10^{-4} Pa. The loading is a simple suspension type, which has the high load stability. The load is monitored by the load cell located in the vacuum chamber, but not controlled electrically from the output of the load cell. The head of the thermocouple is inserted into the hole on the side of the specimen holders to obtain more precise control of the temperature. The heating rate was kept as about 20 K/min and the sample was held for at least 6 hour before the test, to stabilize the outputs from the double linear variable differential transformers (LVDTs) and the load cell. Creep strain was measured by LVDTs, which are connected to Mo specimen holders through Al_2O_3 arms.

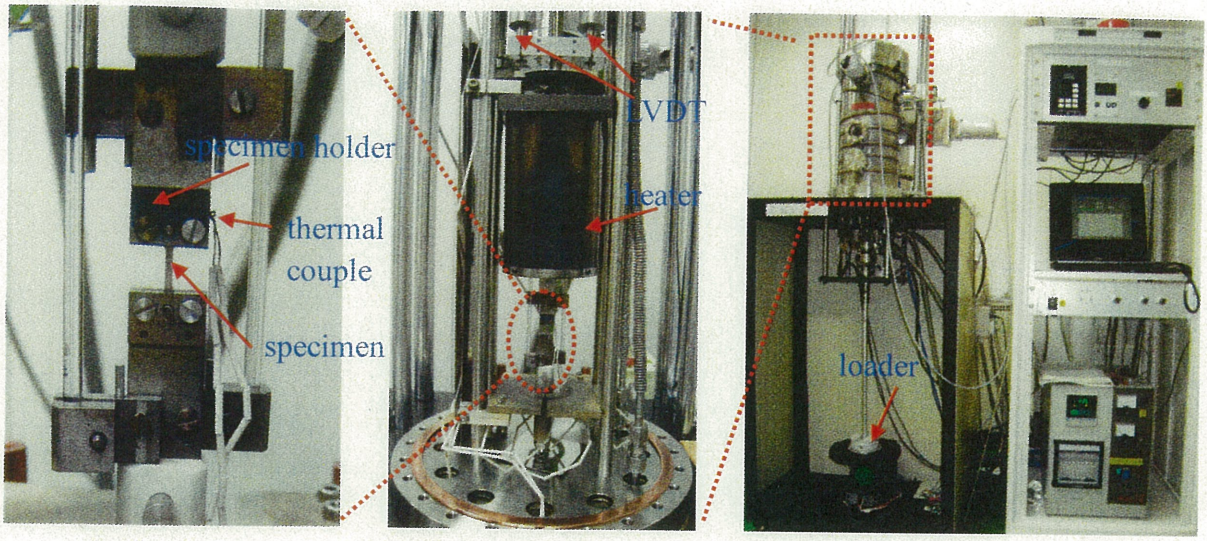

Fig. 2-11 View of the creep property test machine

2.5 Microstructure observation

Many analytical methods were applied to characterization of microstructure after different ageing experiments, including scanning electron microscopy (SEM), electron diffraction spectroscopy (EDS), and transmission electron microscopy (TEM) equipped with energy dispersive X-ray spectroscopy (EDS).

The prior austenite grain was observed by a JEOL-2010S SEM machine with an operated voltage of 20 kV, as shown in *Fig.2-12*. The 3 mm-diameter TEM foils were thinned electrolytically by using a solution of CH_3COOH-$HClO_4$. The observation for precipitates and martensitic laths were done by a JEOL-2000 FX TEM operated at 200 kV at Kyushi University.

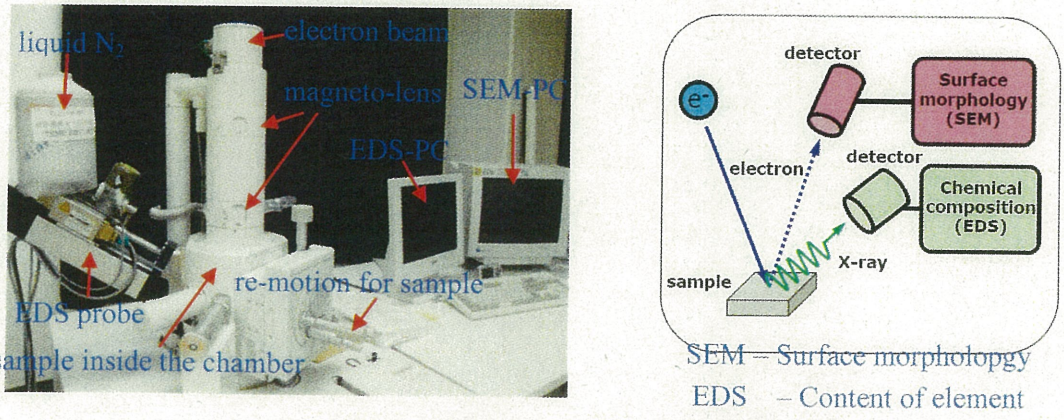

Fig. 2-13 SEM for the microstructure observation

CHAPTER 3

Effects of Thermal Ageing on Mechanical Property of JLF-1 and CLAM Steels

In this section, the effect of thermal ageing on hardness, tensile and creep properties will be reported and discussed.

3.1 Ageing effects on hardness

Hardness is an important mechanical property, which is a measure of a material's resistance to localized plastic deformation.

The ageing effect on Vickers hardness was carried out at RT, and the hardness results before and after ageing are plotted in *Figs. 3-1* and *3-2*. All the measurements were conducted on SS-J or/and small plates with the same thickness and machining condition. For each condition, 5~10 data were tested, and the average values were calculated.

Fig. 3-1 shows the results after ageing for 100 h, compared with those without ageing for JLF-1 and CLAM steels.

With the increase in ageing temperature from 823 to 973 K, the hardness decreased as the general tendency. Compared with that before ageing, the hardness increased slightly for the both steels after ageing at 823 K for 100 h, suggesting ageing-induced hardening. This result is different from that observed in other RAFM steels, which showed that the hardness did not change or decrease during the ageing [79,83]. When ageing temperature was higher than 823 K, the hardness decreased, indicating ageing-induced softening, which is similar to that in other RAFM steels [79,83]. Ageing at 973 K for 100 h caused a significant decrease in hardness, especially for CLAM.

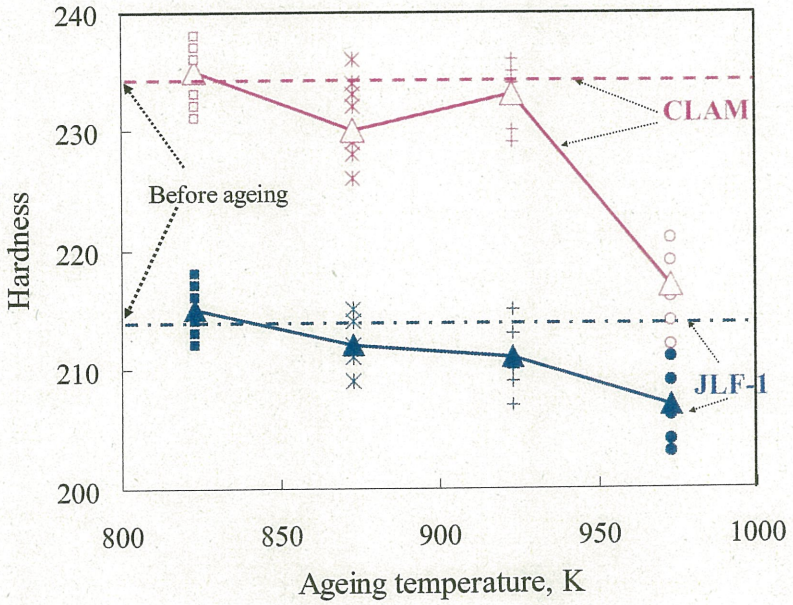

Fig. 3-1 Hardness change of JLF-1 and CLAM steels after ageing for 100 h.

Fig. 3-2 shows the results after ageing for 2000 h. It shows that, after ageing at 823 K for 2000 h, the hardness increased slightly for CLAM and increased remarkably for JLF-1, suggesting ageing-induced hardening. On the contrary, softening occurred above 823 K.

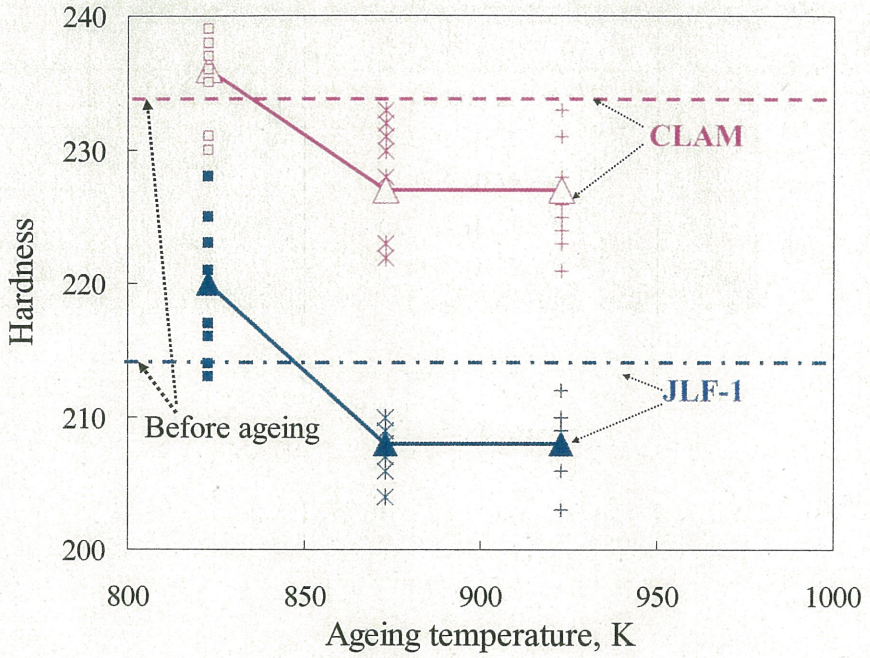

Fig. 3-2 Hardness change of JLF-1 and CLAM steels after ageing for 2000 h.

Comparing these two steels, Figs. 3-1 and 3-2 show that, the hardness of CLAM was higher than that of JLF-1 at all conditions. However, the softening of CLAM was also larger than that of JLF-1 by ageing.

3.2 Ageing effects on tensile properties

3.2.1 Tensile curves

The tensile curves tested at RT, 673, 773, 823 and 873 K for JLF-1 and CLAM steels are presented in *Figs. 3-3 to 3-12*.

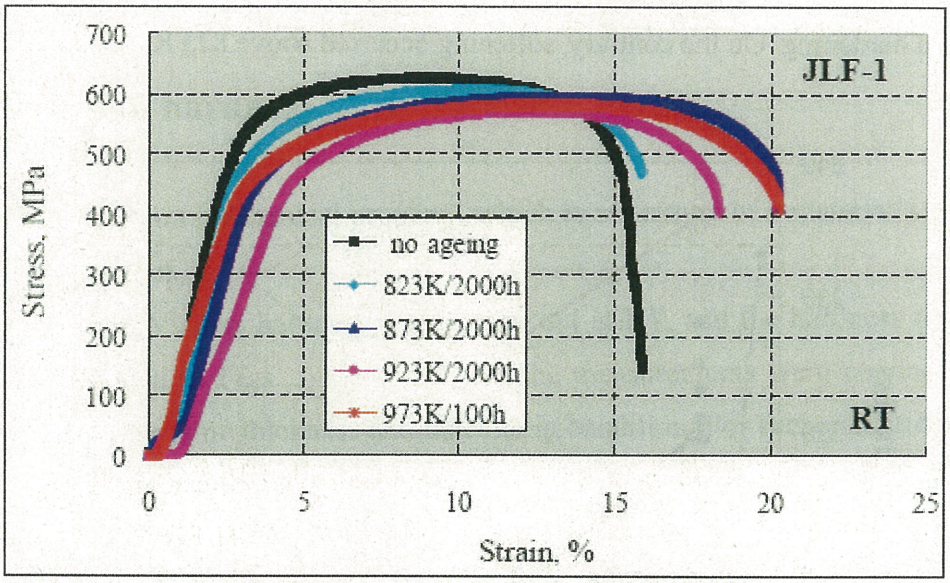

Fig. 3-3 Tensile curves for JLF-1 steel before and after different thermal ageing **(tested at RT)**

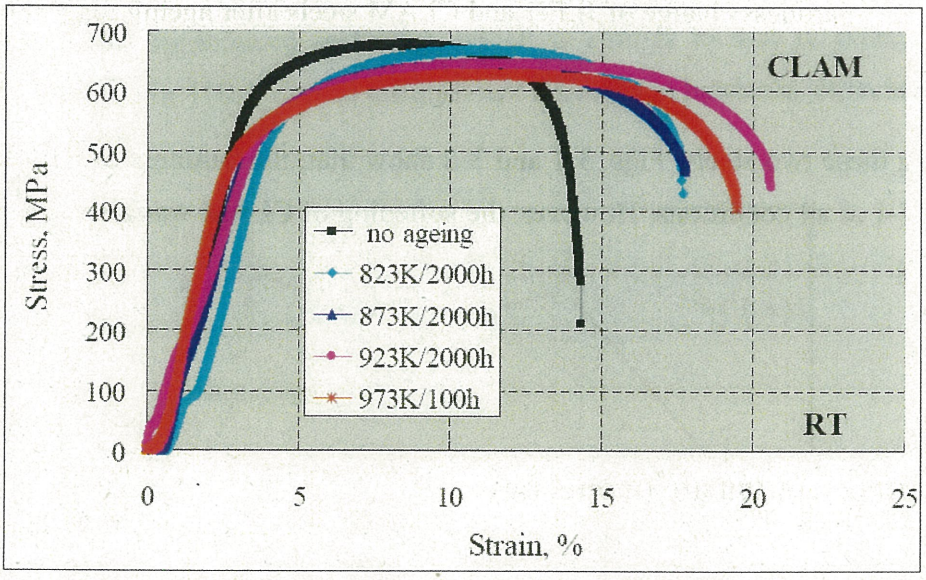

Fig. 3-4 Tensile curves for CLAM steel before and after different thermal ageing **(tested at RT)**

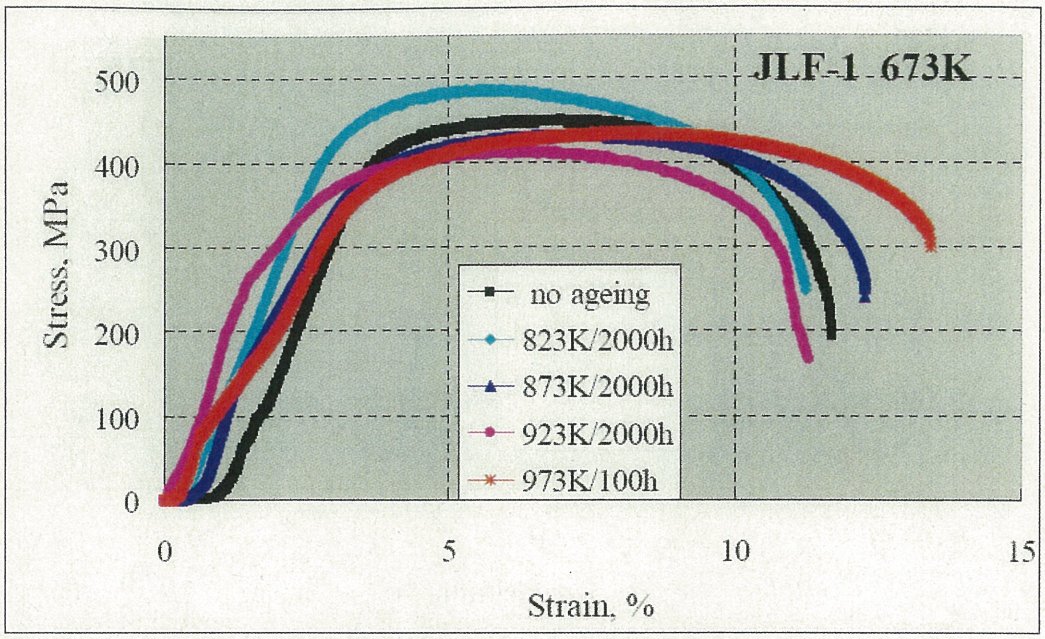

Fig. 3-5 Tensile curves for JLF-1 steel before and after different thermal ageing **(tested at 673 K)**

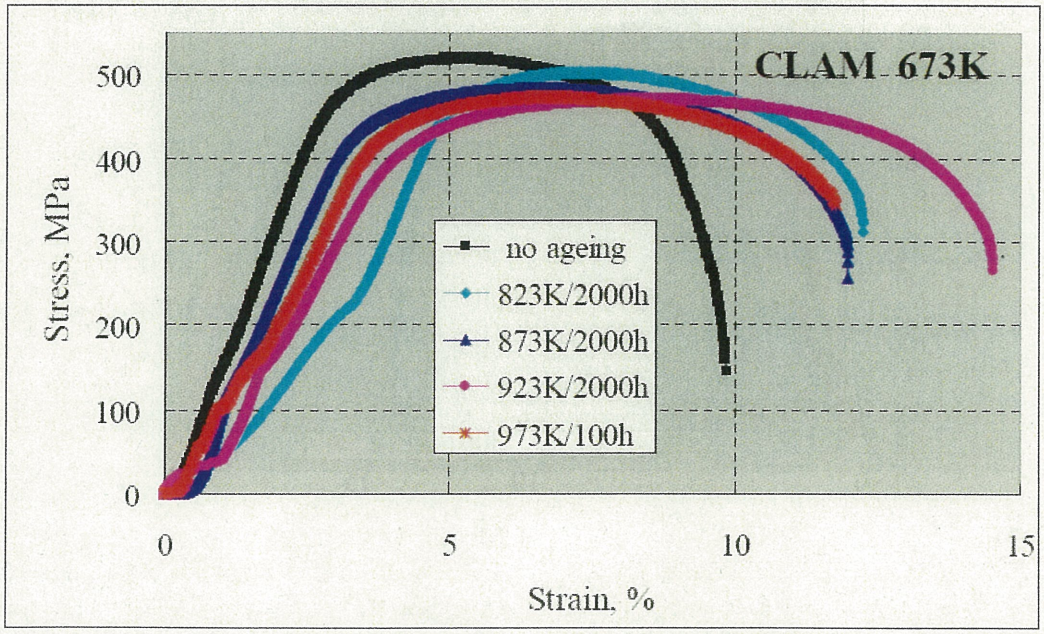

Fig. 3-6 Tensile curves for CLAM steel before and after different thermal ageing **(tested at 673 K)**

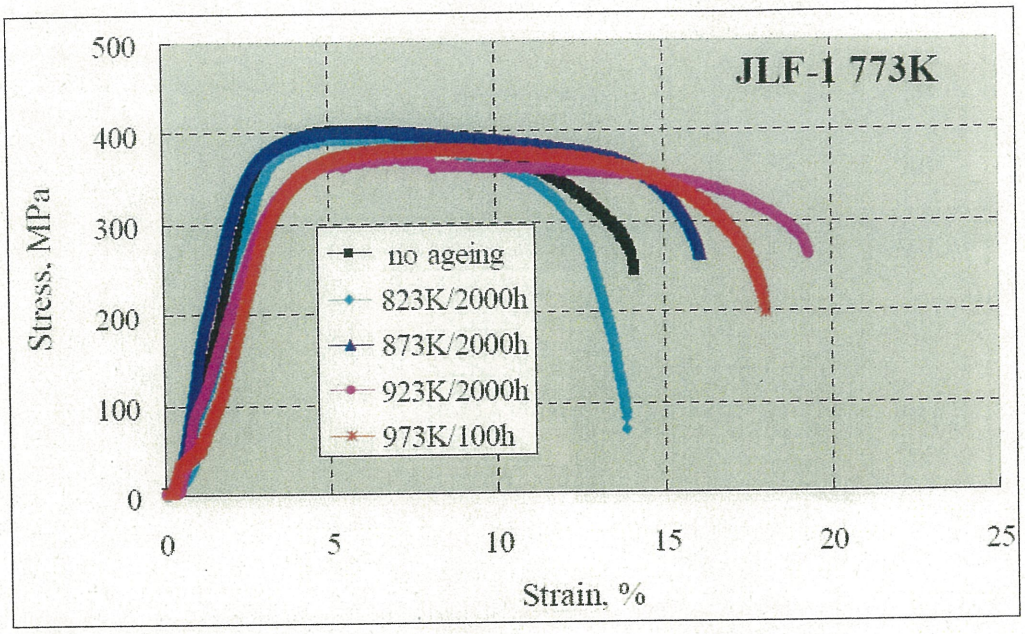

Fig. 3-7 Tensile curves for JLF-1 steel before and after different thermal ageing **(tested at 773 K)**

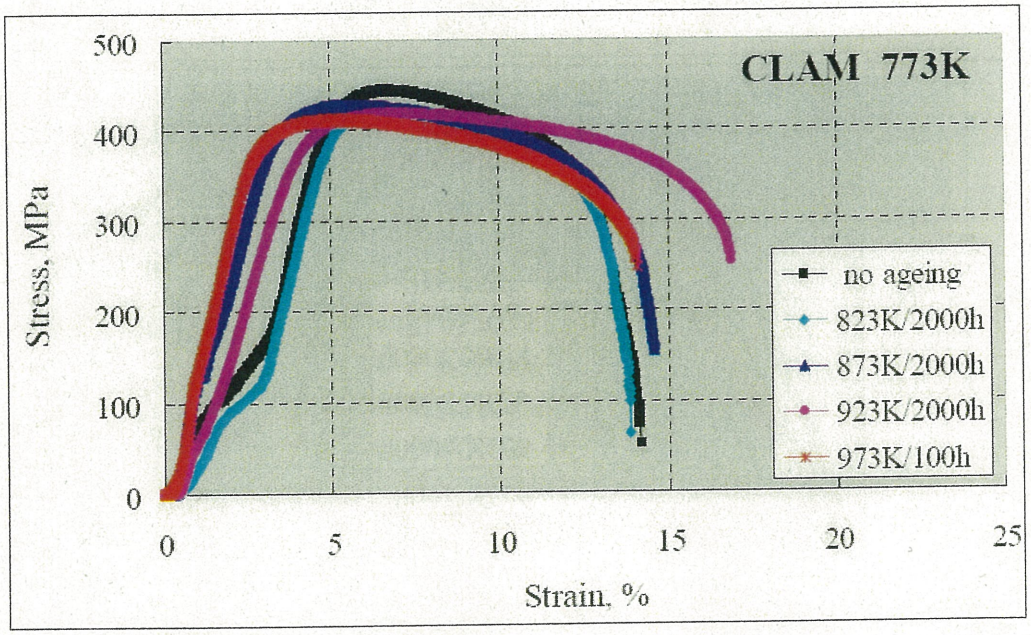

Fig. 3-8 Tensile curves for CLAM steel before and after different thermal ageing **(tested at 773 K)**

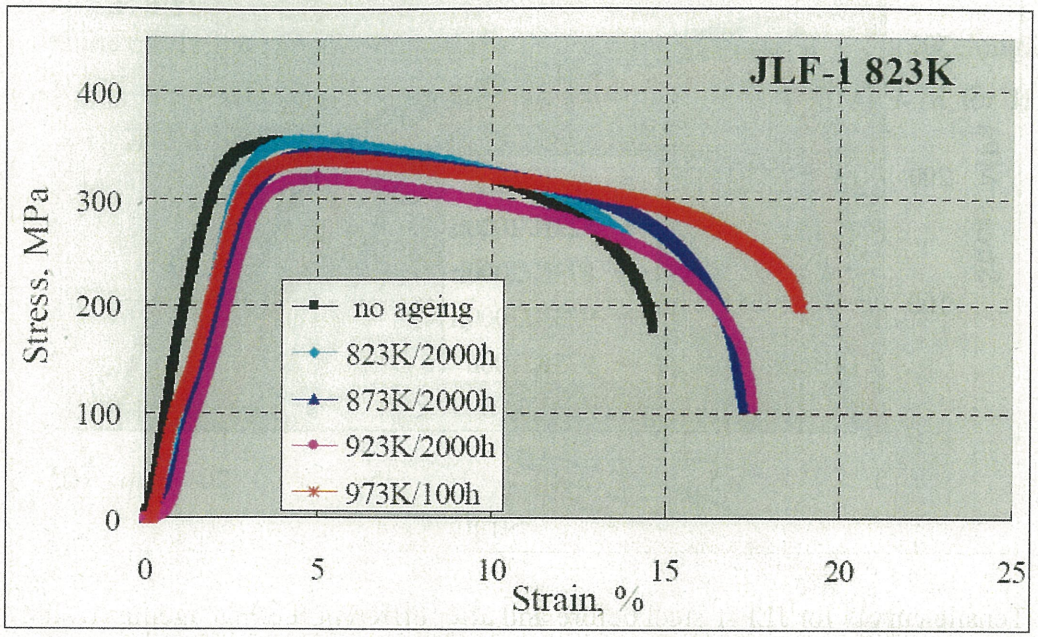

Fig. 3-9 Tensile curves for JLF-1 steel before and after different thermal ageing **(tested at 823 K)**

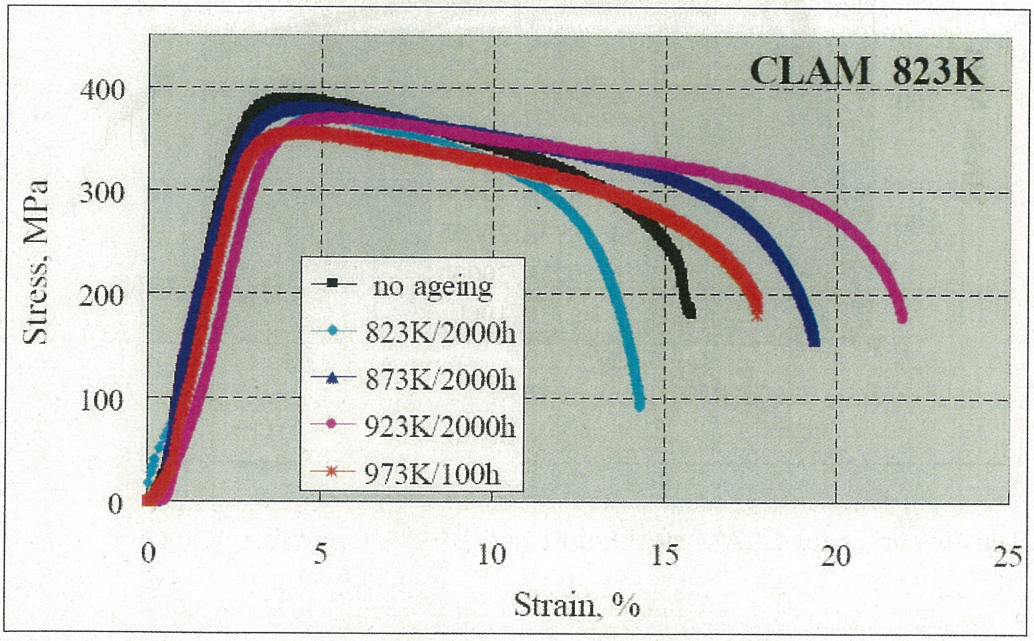

Fig. 3-10 Tensile curves for CLAM steel before and after different thermal ageing **(tested at 823 K)**

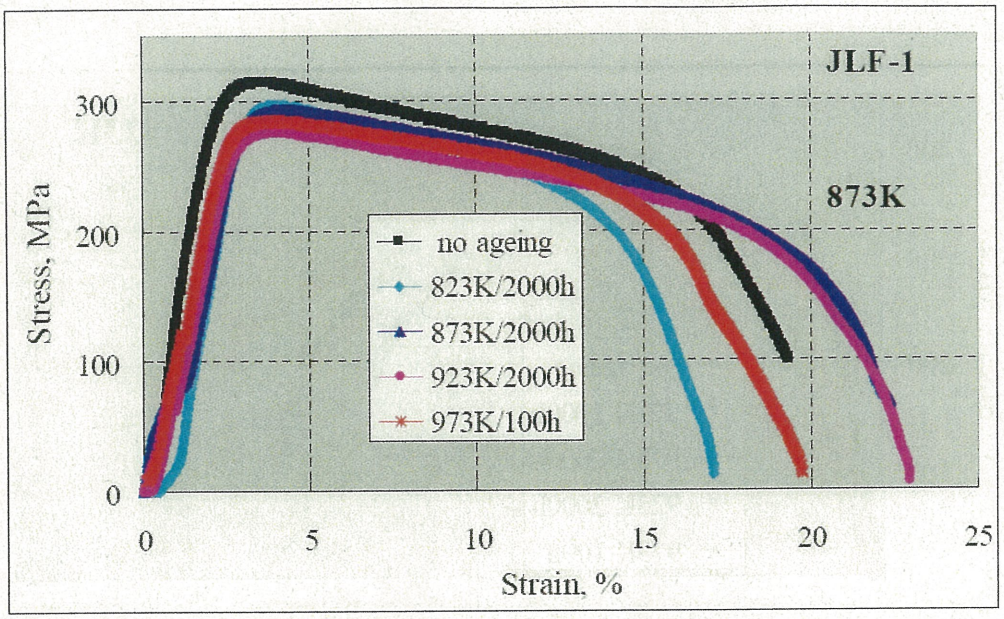

Fig. 3-11 Tensile curves for JLF-1 steel before and after different thermal ageing **(tested at 873 K)**

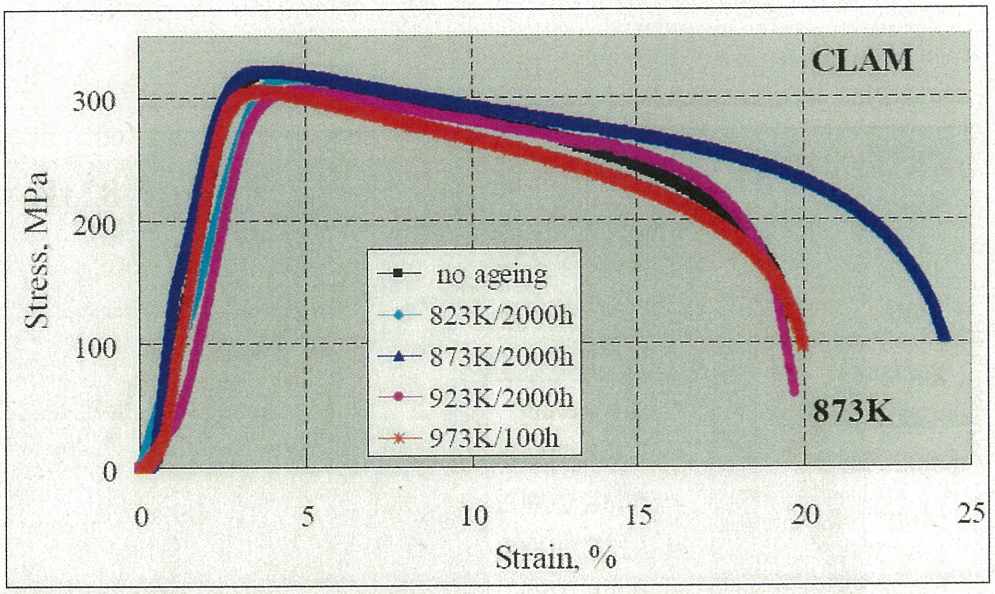

Fig. 3-12 Tensile curves for CLAM steel before and after different thermal ageing **(tested at 873 K)**

The curves shape almost did not change by ageing. With the test temperature increase, the different between the no-aged and aged specimens became small.

From the curves, the ultimate tensile stress, yield stress and total elongation were obtained, which will be reported and discussed in the next section.

3.2.2 Ageing effects on strength and elongation

The results of ultimate tensile strength (UTS), yield strength (YS) and total elongation (TE) in before and after different ageing conditions are shown in *Figs. 3-13 to 3-18* for JLF-1 and CLAM.

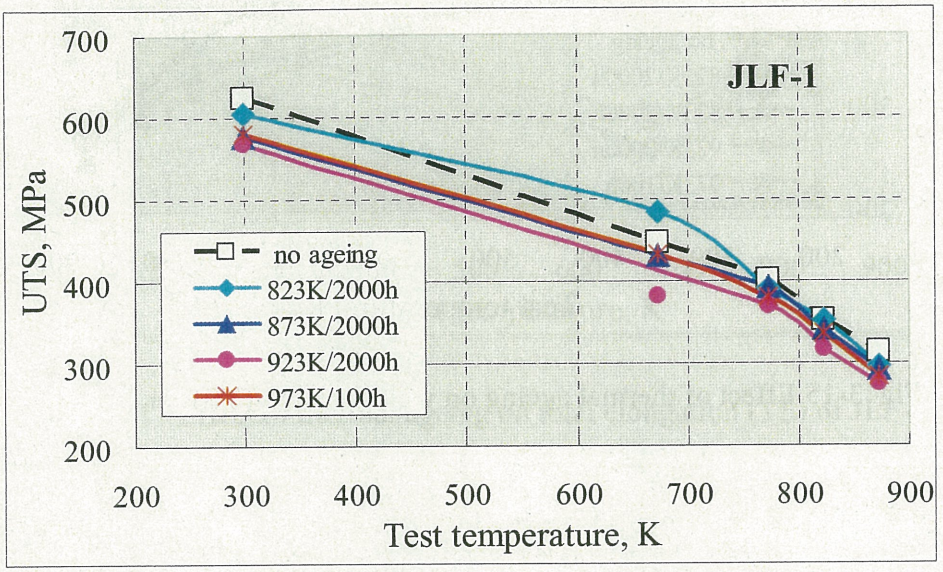

Fig. 3-13 Effect of thermal ageing on ultimate tensile strength (UTS) for JLF-1

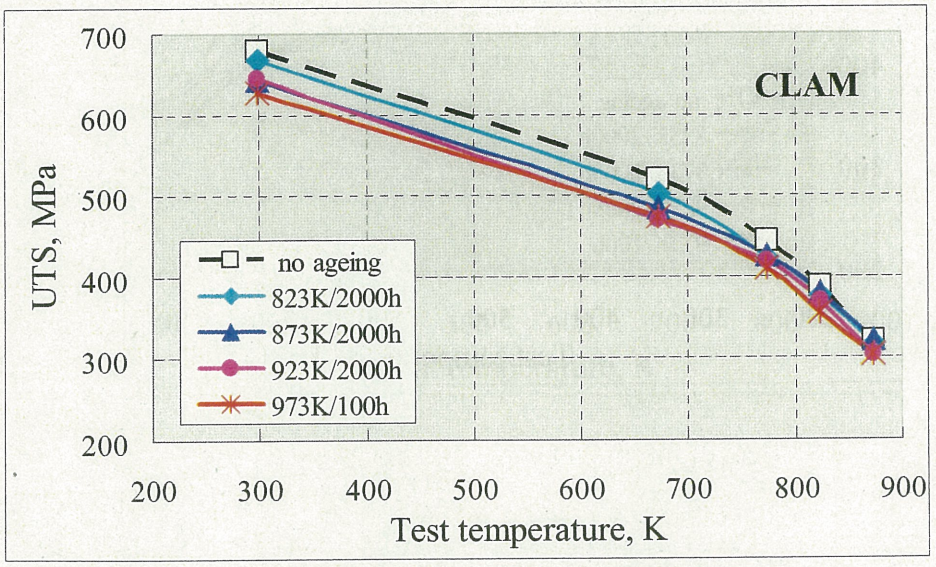

Fig. 3-14 Effect of thermal ageing on ultimate tensile strength (UTS) for CLAM

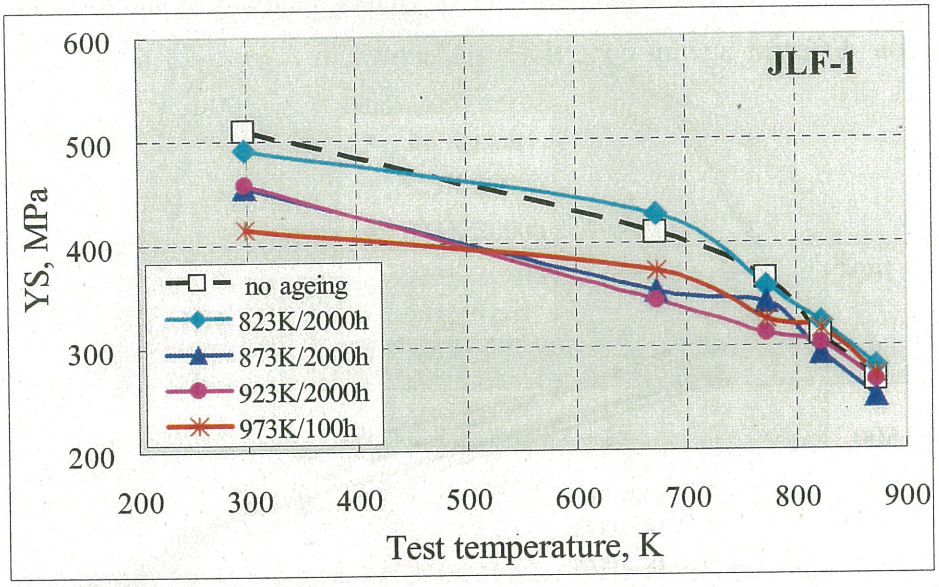

Fig. 3-15 Effect of thermal ageing on yield strength (YS) for JLF-1

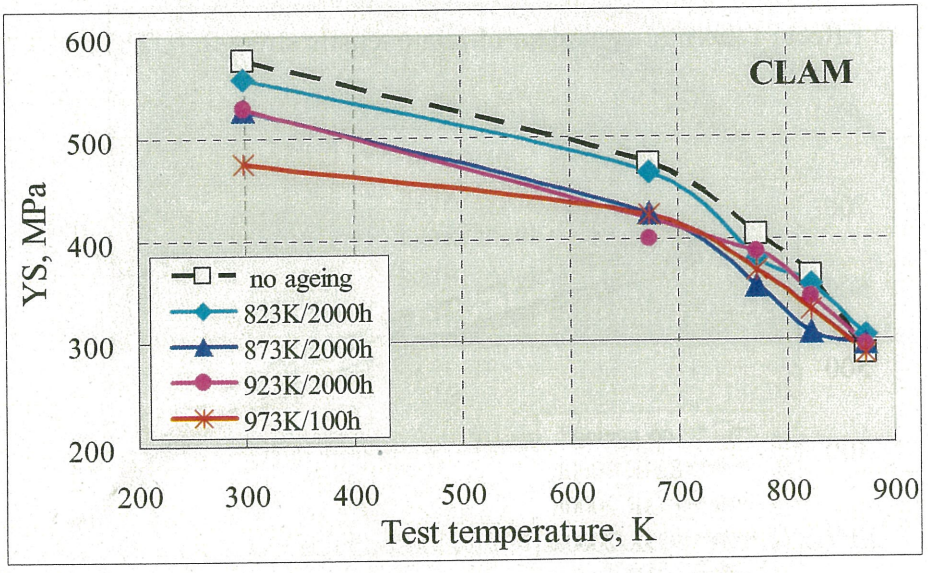

Fig. 3-16 Effect of thermal ageing on yield strength (YS) for CLAM

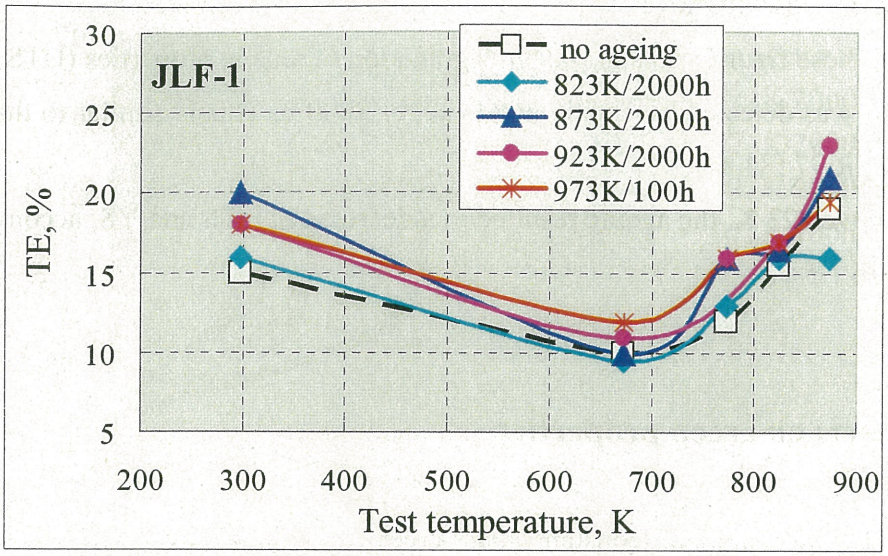

Fig. 3-17 Effect of thermal ageing on total elongation (TE) of JLF-1

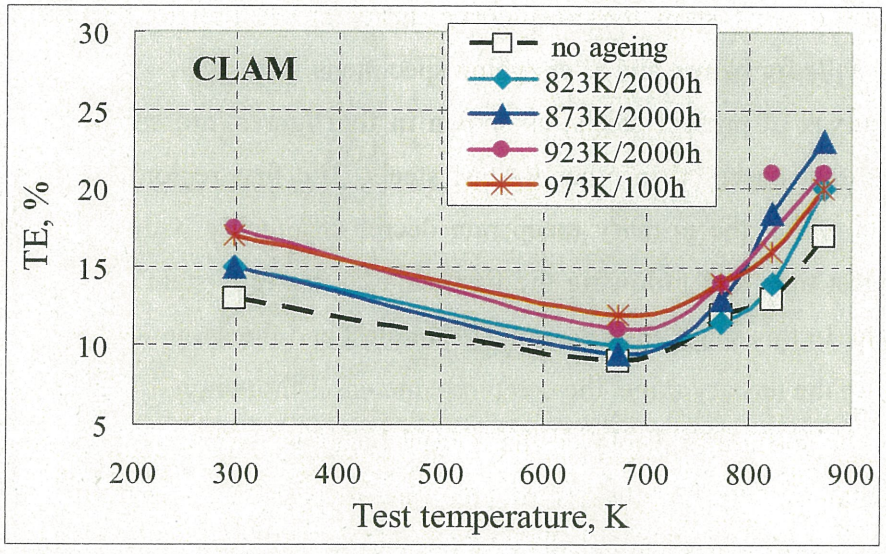

Fig. 3-18 Effect of thermal ageing on total elongation (TE) for CLAM

The UTS and YS of CLAM were higher and TE was smaller than those of JLF-1, in agreement with the hardness data. Compared with other RAFM steels, the both steels exhibit adequate strength and ductility level [62,90].

As shown in these figures, no significant degradation of tensile properties (UTS, YS and TE) for the both steels was detected by ageing at 823 K for 2000 h. This is similar to those for F82H [83] and EUROFER 97 [84,86].

However, above 823 K, the ageing resulted in a decrease in UTS and YS, accompanied by an increase slightly in TE.

3.3 Ageing effects on creep properties

In this study, the uniaxial constant load creep to rupture experiments were conducted systemicaly at the tempearture range from 823 to 973 K with the applied stresses between 100 and 300 MPa.

3.3.2 Creep curves of JLF-1 and CLAM

The *Figs. 3-19 to 3-24* show the creep curves tested at 823 K with different applied stress of 220, 250 and 300 MPa for before and after ageing specimens.

The creep curves of present steels, as shown in the figures, are composed of three distinct regions similar to that observed in other RAFM steels. The first region is the primary creep, or transient creep, in which the primary creep rate decreases quickly with time. The second stage occupies the longest time and following the first stage, is a steady-state creep, characterized by a constant creep rate. In this stage, the creep rate is smallest and the strain increases very slowly with time. Eventually, in the tertiary stage, the creep rate increases more rapidly until the sample failed.

In all cases, the specimens displayed the normal behavior with respect to the applied stress, where at any constant temperature the deformation rate increased and the secondary stage became less pronounced with the increase of the applied stress.

Clearly, the thermal ageing affected the shape of creep curves for the both steels. The effect was remarkably at lower stress range and for CLAM.

The effects on the important creep parameters, minimum creep rate and rupture time, will be discussed in detail in the next section.

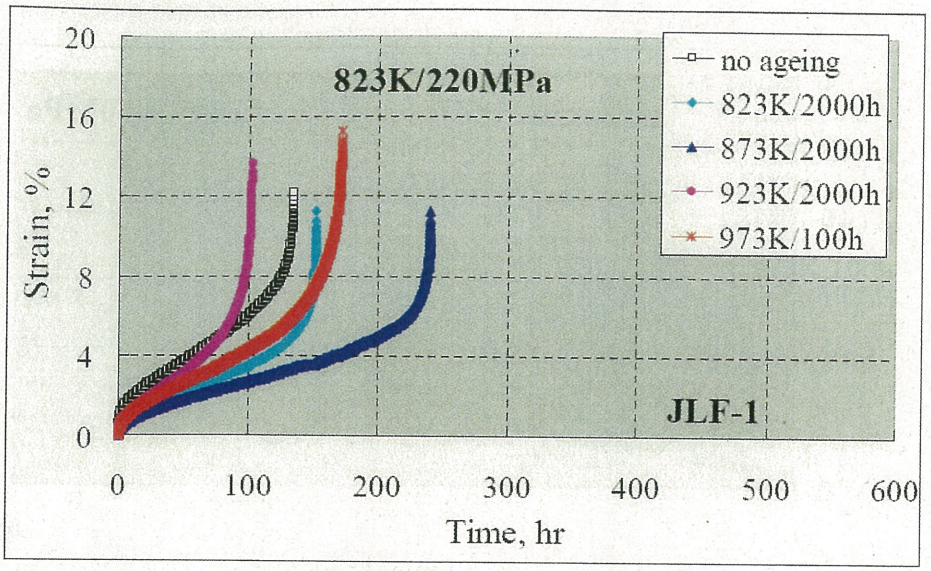

Fig. 3-19 Ageing effects on creep curves of JLF-1 steel (tested at **823K/220MPa**)

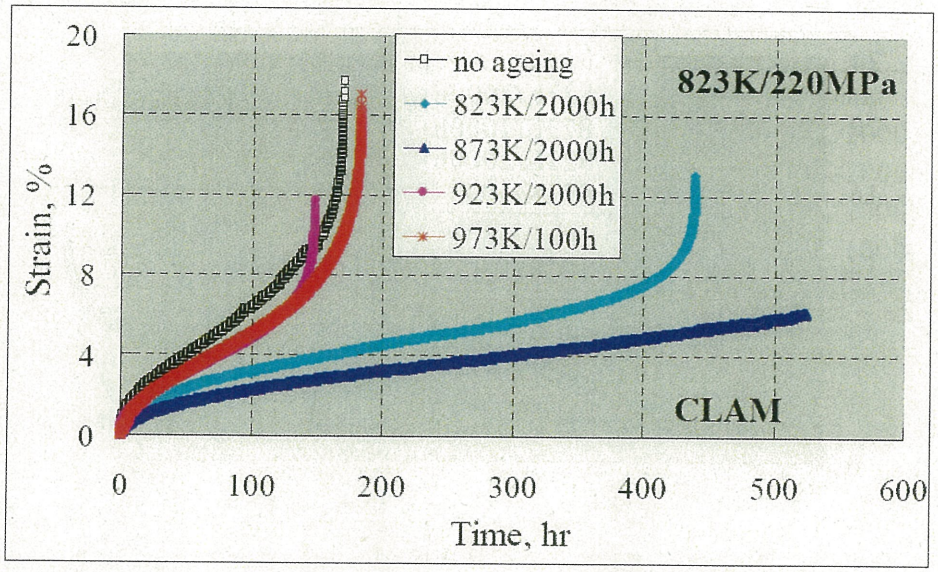

Fig. 3-20 Ageing effects on creep curves of CLAM steel (The sample aged at 873k/2000h did not run to rupture) (tested at **823K/220MPa**)

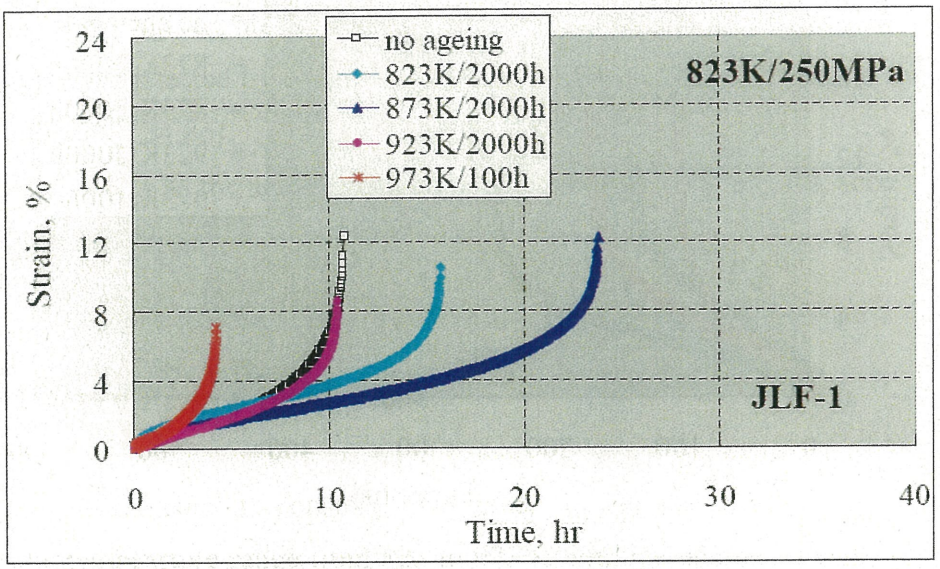

Fig. 3-21 Ageing effects on creep curves of JLF-1 steel (tested at **823K/250MPa**)

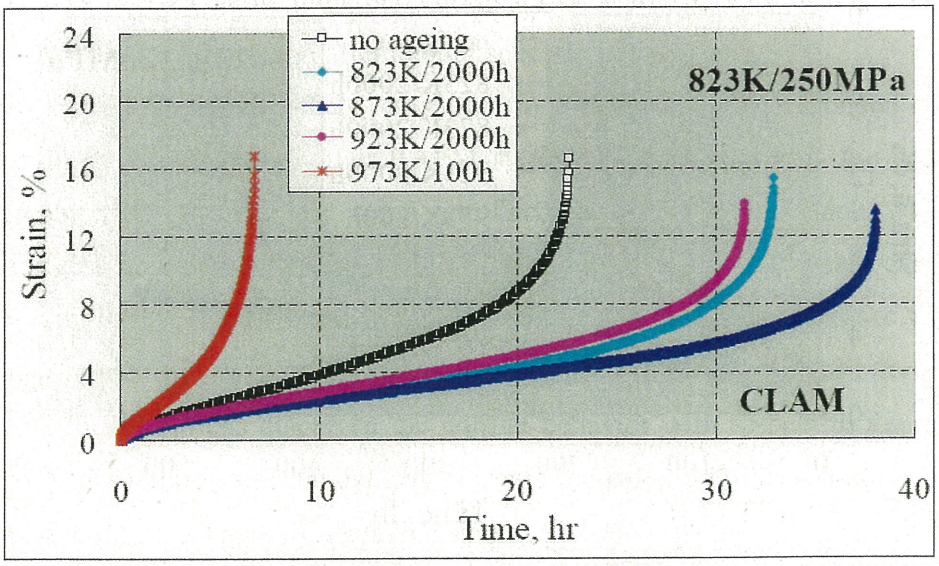

Fig. 3-22 Ageing effects on creep curves of CLAM steel (tested at **823K/250MPa**)

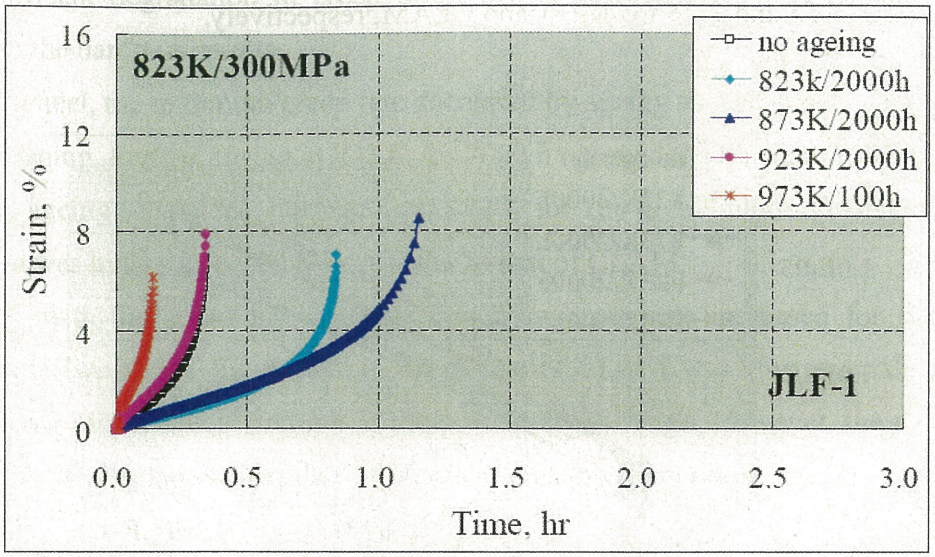

Fig. 3-23 Ageing effects on creep curves of JLF-1 steel (tested at **823K/300MPa**)

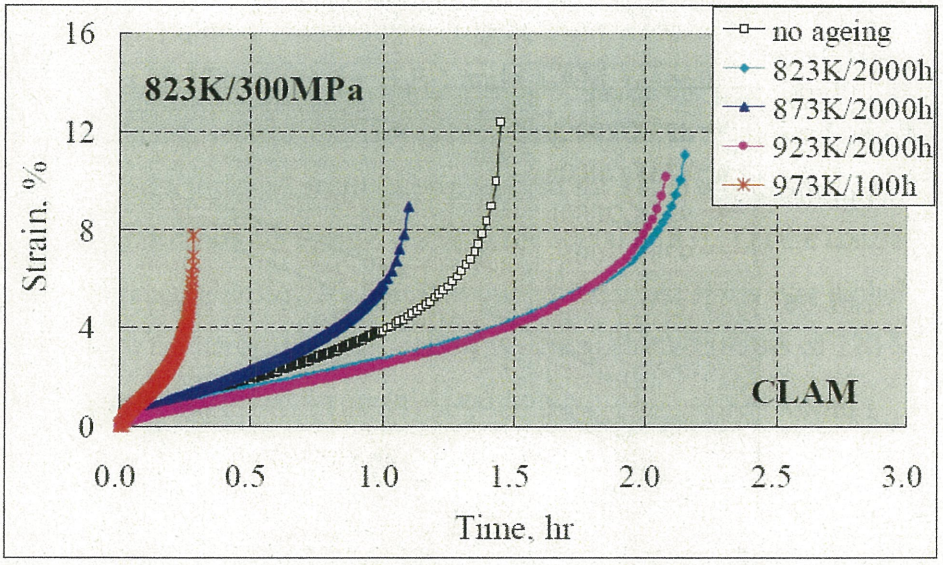

Fig. 3-24 Ageing effects on creep curves of CLAM steel (tested at **823K/300MPa**)

3.3.2 Ageing effect on minimum creep rate

From the second stage of creep curves, the minimum creep rate was obtained by linear regression analysis. The results of minimum creep rate tested at 823 K with different stresses are summarized in *Figs. 3-25* and *3-26* for JLF-1 and CLAM, respectively.

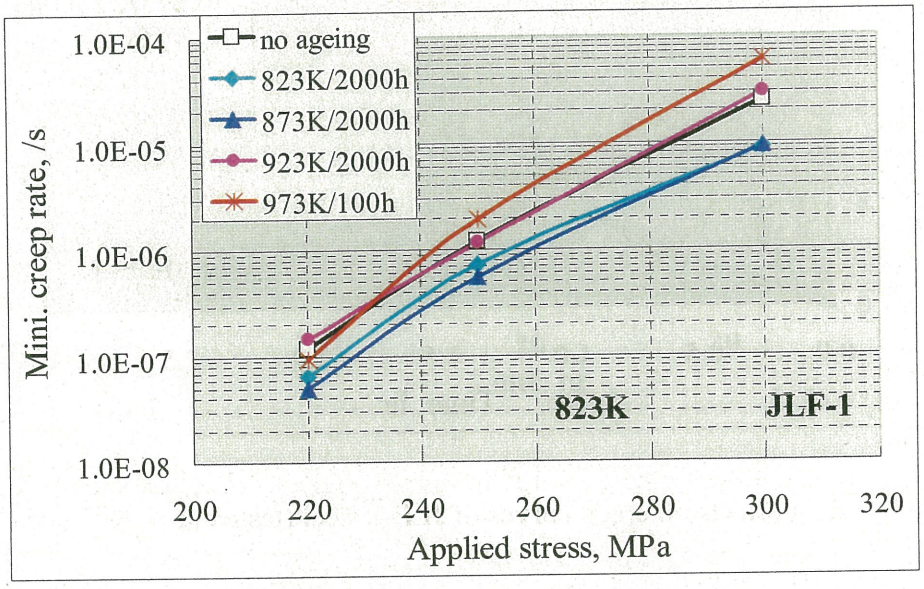

Fig. 3-25 Ageing effects on minimum creep rate for JLF-1 steel (tested at **823K**)

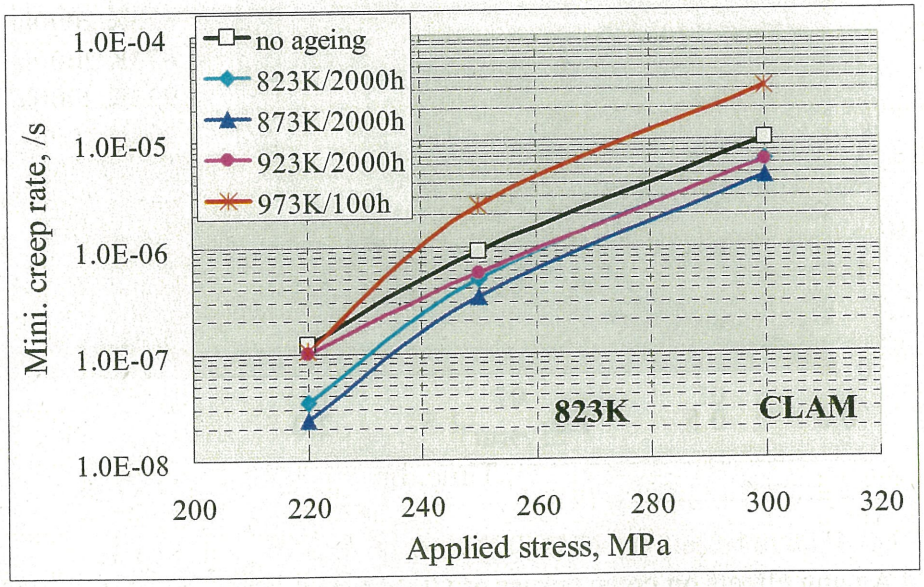

Fig. 3-26 Ageing effects on minimum creep rate for CLAM steel (tested at **823K**)

For CLAM steel, the minimum creep rate decreased by ageing at 823 to 923 K up to 2000 h, suggesting hardening. This hardening phenomina was firstly observed, and different from the typical softening obtained for other RAFM steels [87]. On the other hand, ageing at 973 K for 100 h caused a significant degradation in creep properties at stress higher than 220 MPa, which are consistent with the hardness results.

For JLF-1 steel, the minimum creep rate decreased by ageing at 823 and 873 K for 2000 h, also indicating hardening. Further ageing at 923 K for 2000 h returned the minimum creep rate to almost the level of no ageing specimens. For ageing at 973 K for 100 h, the minimum creep rate degraded when the stress was higher than 220 MPa, similar to that of CLAM.

Generally, with the stress increase, the minimum creep rate increased for the both steels. Comparing these two steels, the minimum creep rate of CLAM was always smaller than that of JLF-1, suggesting higher creep strength at the present stress range. However, the change in creep rate by ageing was also larger than that of JLF-1, indicating higher suscepitility to thermal ageing than that of JLF-1.

3.3.3 Ageing effects on rupture time

From the tertiary stage of creep curves, the rupture time was measured, which is the total time for the specimen to rupture. The results of rupture time tested at 823 K with different stresses are summarized in *Figs. 3-27* to *3-28*, for JLF-1 and CLAM, respectively.

The rupture time increased for CLAM after ageing at 823 to 923 K up to 2000 h, implying hardening. This results are different from those observed for F82H steel, which showed the rupture time was decreased significantly by ageing at 873 K for 30000 h [87]. On the contray, ageing at 973 K for 100 h caused a remarkable degradation in rupture time when stress was higher than 220 MPa, which is consistent with the hardness results. Howeve, creep at lower stress of 220 MPa, the rupture time returned to alomost the level of no ageing condition.

For JLF-1 steel, the rupture time increased after ageing at 823 and 873 K for 2000 h, suggesting hardening. Further ageing at 923 K for 2000 h returned the properties to almost the level of no ageing. Ageing at 973 K for 100 h caused a significant degradation of rupture time when stress were 250 and 300 MPa. During the longer-time creep with lower stress of 220 MPa, the rupture time did not decrease but increase.

Comparing these two steels, the rupture time of CLAM was longer than that of JLF-1. However, CLAM was more susceptible to thermal ageing than that of JLF-1.

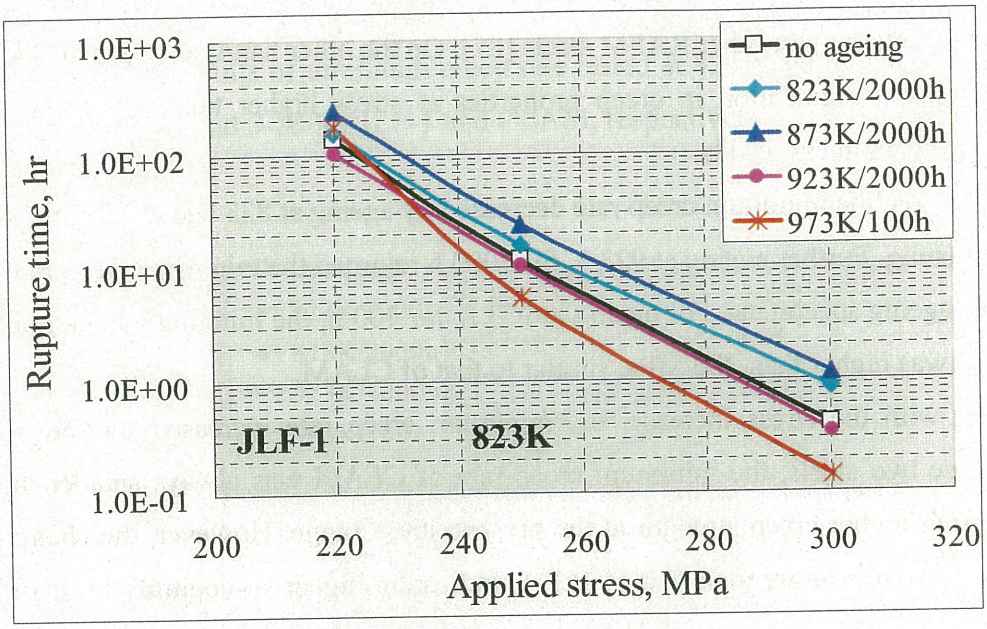

Fig. 3-27 Ageing effect on rupture time for JLF-1 (tested at **823 K**).

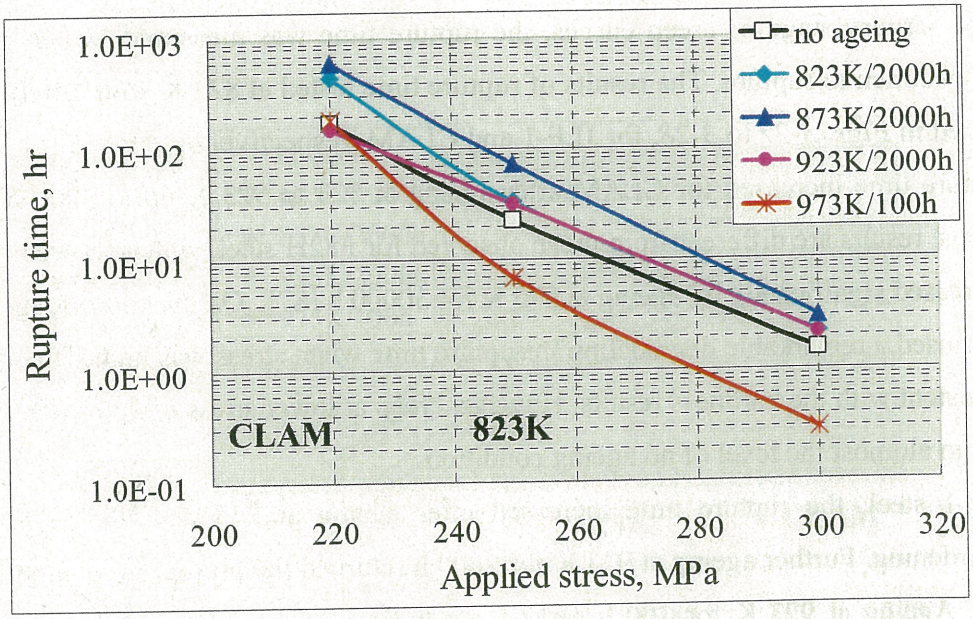

Fig. 3-28 Ageing effect on rupture time for CLAM (tested at **823 K**).

3.4 Discussion

3.4.1 Mechanism of creep

The mechanism of creep depends on temperature and stress. Generally, there are three basic mechanisms of creep in metals as followed:

(a) Dislocation creep [91-92]

At high stresses (relative to the shear modulus), creep is controlled by the movement of dislocations. When a stress is applied to a material, plastic deformation occurs due to the movement of dislocations in the slip plane. Materials contain a variety of defects, for example solute atoms, that act as obstacles to dislocation motion. At high temperatures vacancies in the crystal can diffuse to the location of a dislocation and cause the dislocation to move to an adjacent slip plane, which is called climbing. By climbing to adjacent slip planes dislocations can get around the obstacles to their motion, allowing further deformation to occur.

Dislocation creep rate has a strong dependence on the applied stress and is influenced weekly by grain size. The dislocation creep also called power-law creep.

(b) Diffusion creep [91-92]

At relative low stress and high temperature, the creep is significantly controlled by the diffusion process. Under the driving force of the applied stress, atoms diffuse and cause the grains to elongate along the stress axis.

For diffusion path through the grains, the mechanism is called Nabarro-Herring (N-H) creep, which usually takes place at 0.7 T_m and above. In this case, the atoms have a slower jump frequency but more paths.

For diffusion path along the grain boundaries, the mechanism is called Coble creep, where the jump frequency is higher but fewer paths exist. Coble creep occurs at lower temperatures than that of N-H creep.

(c) Grain boundary sliding creep

At high temperature and low strain rate creep, the diffusion of atoms in grain boundaries becomes easy. Thus, the sliding of grain boundary occurs when the shear stresses act on the boundaries.

The deformation-mechanism map was developed for many kinds of metals. The schematic illustration of the deformation-mechanism map by Ashby is shown in *Fig. 3-29* [91], providing an overview of the deformation mechanism of a material under a given temperature and stress.

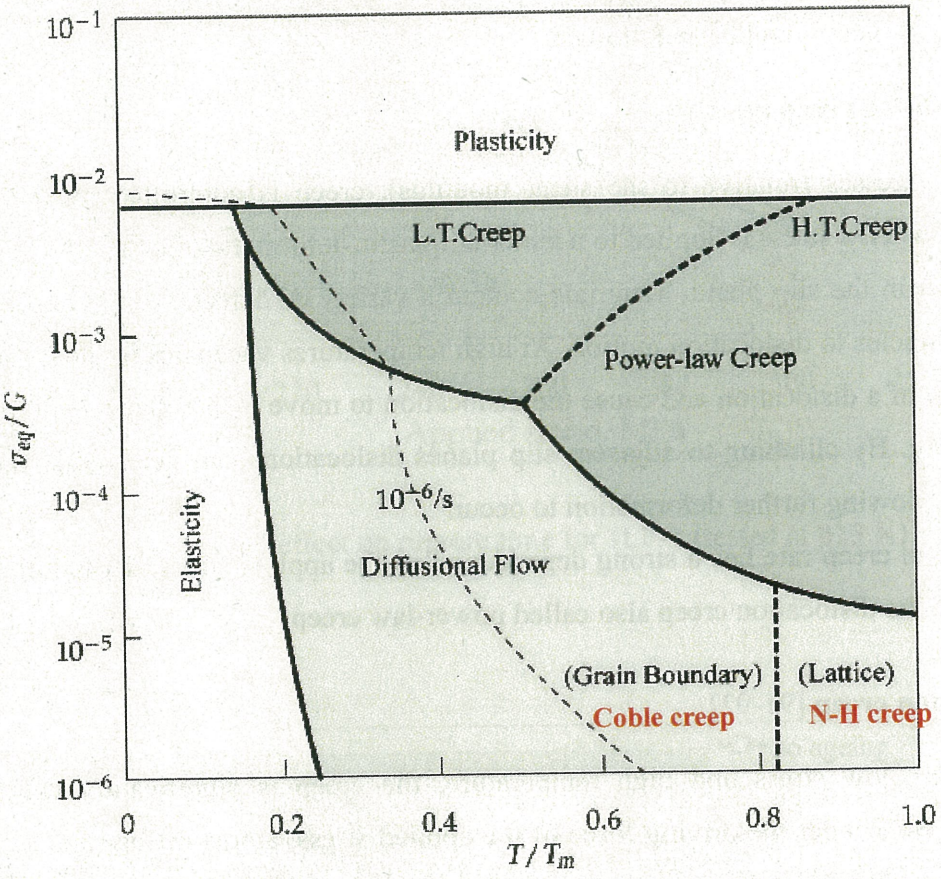

Fig. 3-29 Schematic deformation-mechanism map by Ashby (T_m: the melting temperature, G: shear modulus, L.T.Creep: low temperature creep, and H.T. Creep: high temperature creep) [91]

3.4.2 Power-law equation

Generally, the minimum creep rate can be described by a traditional power-law equation (also called Norton equation) as followed [91]:

$$r_{\min} = \frac{d\varepsilon}{dt} = k\sigma^n \qquad (3\text{-}1)$$

where

r_{min}, $\frac{d\varepsilon}{dt}$: minimum creep rate

k: constant

σ: applied stress

n: Norton stress exponent

Taking the logarithm for the both sides of equation 3-1, then:

$$\log r_{min} = \log k + n \log \sigma \qquad (3\text{-}2)$$

Thus, the minimum creep rate (r_{min}) shows a linear function of the applied stress (σ) in log-log scale for each test temperature. From this slope, the stress exponent n can be determined.

It is well known that the value of stress exponent n varies in a large range, strongly dependent on the material, temperature, and the imposed stress in the creep conditions [91-93]. Thus a change of n is indicative of a change in mechanism of creep deformation. When the creep is controlled by dislocation process, the stress exponent n is usually equal to 3~5, as proved in many pure metals and single-phase alloys displaying normal creep curves at high temperatures [91, 94]. When the creep mechanism is shifted from dislocation to diffusion creep, n will decrease to about 1 [91-92, 94].

However, n is frequently found to higher than 3-5 in many materials controlled by dislocation creep. For example, n was equal to 6-8.7 in 9Cr-1Mo steel [95], and 13.8 in 9Cr-2W steel [96]. In addition, in the alloys which are strengthened by a dispersion of fine precipitates and/or insoluble particles, the observed n value can be remarkably greater than the materials without particles. It was reported that n was equal to 50 for the MA957 ODS steel (Fe-14Cr-2.2Ti-0.3Mo-0.3wt%Y_2O_3) tested at 923 to 973 K [97].

The results of minimum creep rate versus applied stress are plotted in the *Figs. 3-30* and *3-31* for JLF-1 and CLAM before ageing, respectively. Based on the linear regression analysis, the exponent n was determined for temperature from 823 to 923 K.

The figures showed that, with the increase in test temperature from 823 to 923 K, stress exponent n varied from 18 to 11 and 14 to 10 for JLF-1 and CLAM, respectively. All the obtained n was higher than the typical value of 3 ~ 5, suggesting the particle-strengthened dislocation creep.

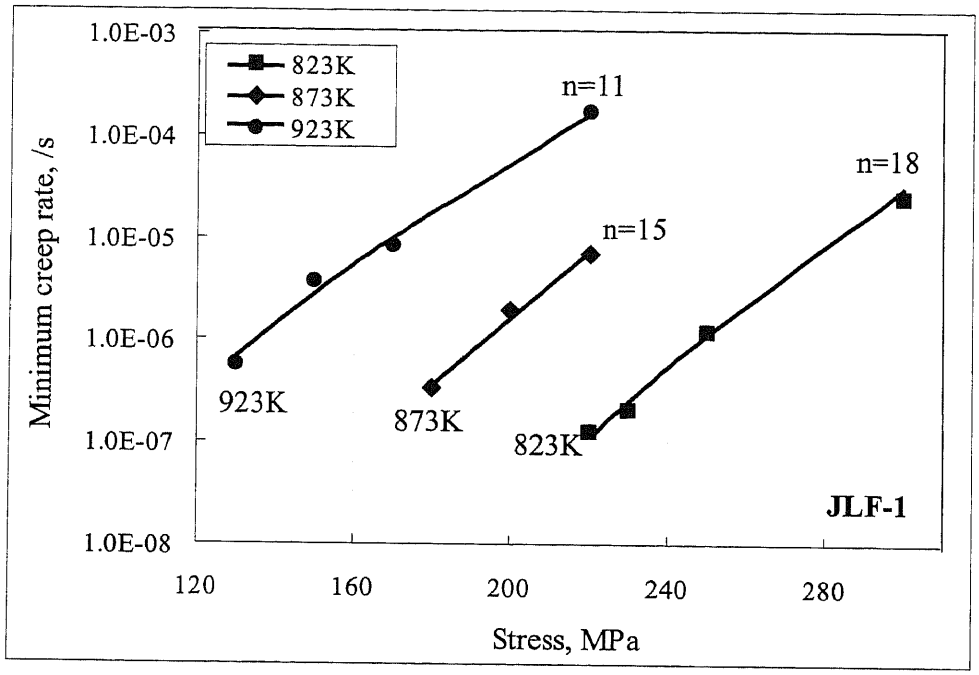

Fig. 3-30 Minimum creep rate vs. the applied stress for JLF-1 steel before ageing (from the lines slope the stress exponent n can be determined at each test temperature from 823 to 923 K).

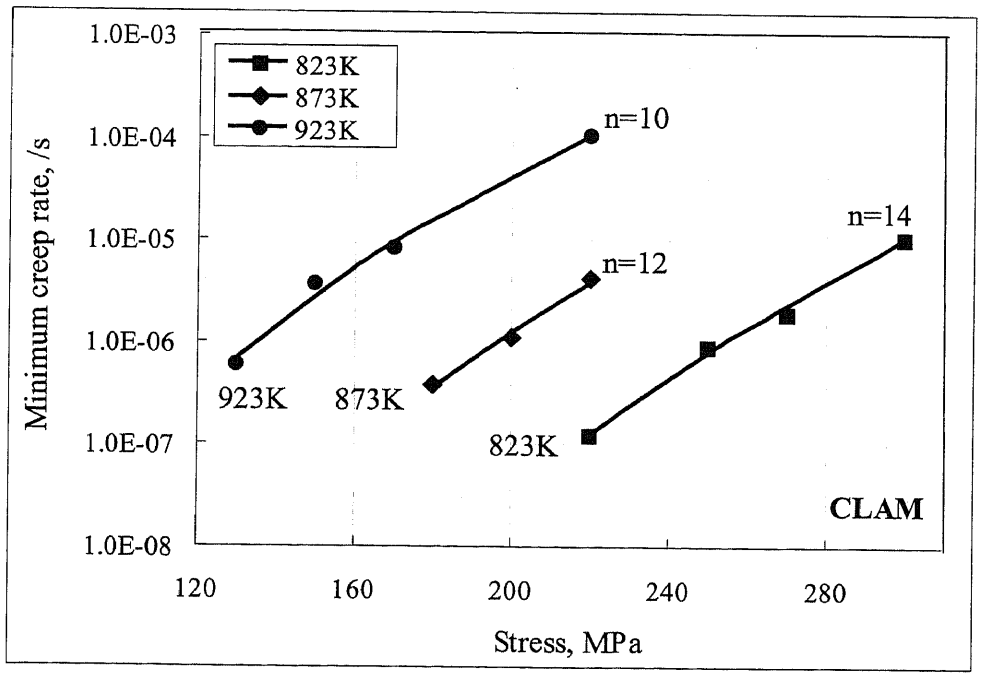

Fig. 3-31 Minimum creep rate vs. the applied stress for CLAM steel before ageing (from the lines slope the stress exponent n can be determined at each test temperature from 823 to 923 K).

In addition, figures showed a strong linear dependence of minimum creep rate (r_{min}) on the applied stress (σ), and almost no change in slope (n) was observed at each test temperature. This indicates that the both steels were controlled by a unique creep mechanism during the present stress range.

The summary of all n values is shown in *Table 3-1*. The results for other RAFM steels are also listed here for comparison [86]. It showed that the exponent stress n for JLF-1 and CLAM are comparable to other RAFM steels.

Table 3-1 Stress exponent (n) values for several kinds of RAFM steels

Steel	Heat treatment	Temperature, K	n	Stress range, MPa
JLF-1	1313K + 1053K	823	18	220-300
		873	15	180-220
		923	11	130-200
CLAM	1253K + 1033K	823	14	220-300
		873	12	180-220
		923	10	130-200
EUROFER 97 [86]	1253K + 1013-1033K	823	18	170-220
		873	10	100-160
		923	6.2	50-90
F82H-mod [86]	1223-1273K + 1023K	823	18	170-220
		873	12.5	100-160
		923	8.4	50-90

The ageing effects on the value of stress exponent n have also been studied in this study, and the results are shown in *Figs. 3-32* and *3-33* for JLF-1 and CLAM, respectively. For comparison, the data before ageing are also shown.

After ageing at 823 K for 2000 h and 973 K for 100 h, no remarkable change in n occurred for the both steels at test temperature of 823 K. It implies that no significant change in creep mechanism took place during the present ageing.

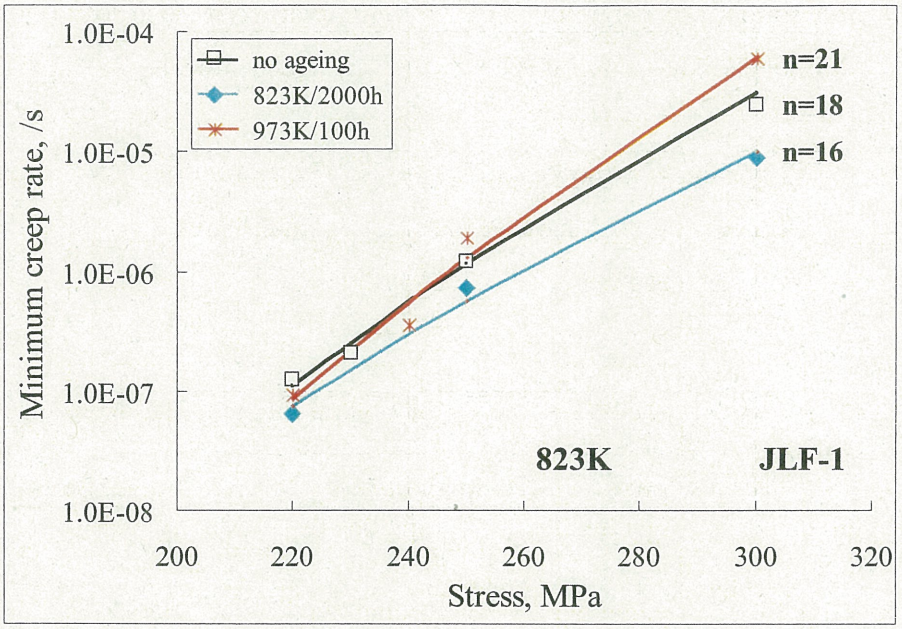

Fig. 3-32 Minimum creep rate vs. applied stress for JLF-1 steel after ageing, compared with that no ageing (from the slope the stress exponent n can be determined at test temperature of 823 K)

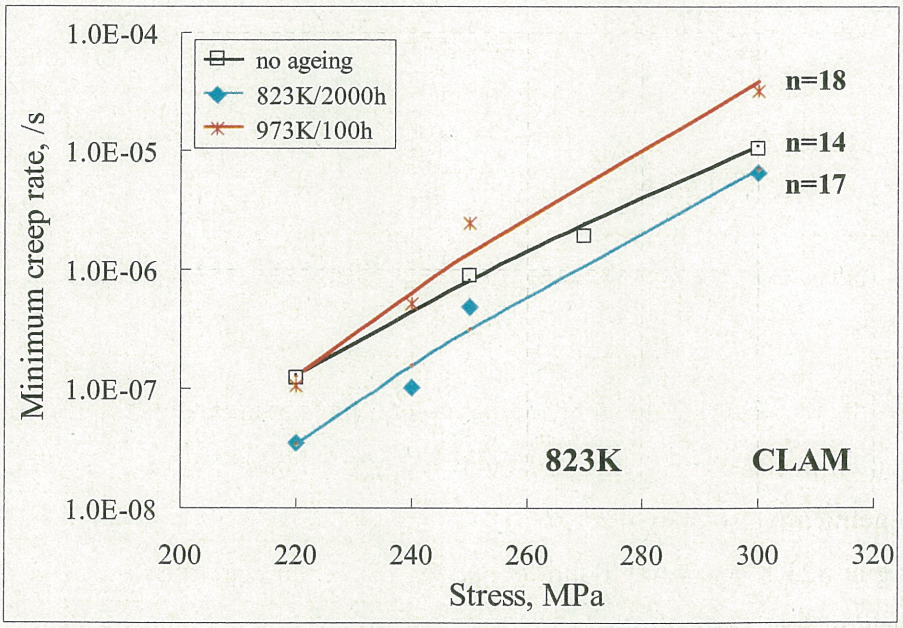

Fig. 3-33 Minimum creep rate vs. applied stress for JLF-1 steel after ageing, compared with that no ageing (from the slope the stress exponent n can be determined at test temperature of 823 K)

3.4.3 Activation energy for creep deformation

The temperature dependence of creep can be traditionally characterized by activation energy, Q. The relation of minimum creep rate with temperature is described by Arrhenius equation [91]:

$$r_{\min} = \frac{d\varepsilon}{dt} = A\exp\left(-\frac{Q}{RT}\right) \qquad (3\text{-}3)$$

where

r_{min}: stead-state creep rate, or minimum creep rate

A: constant

Q: apparent activation energy, J

exp: logarithm

R: gas constant, 8.314 J/mol.K

T: temperature, K

Based on this equation, if the structure is assumed not to change over the temperature change, Q can be obtained by the related test temperatures T_1 and T_2, and corresponding minimum creep rate $r_{min,1}$ and $r_{min,2}$:

$$Q = R(\ln r_{\min,1} - \ln r_{\min,2})/(1/T_2 - 1/T_1) \qquad (3\text{-}4)$$

Generally, for dislocation creep, the activation energy Q is close to the energy for self-diffusion [91,94]. However, it was reported that, similar to the stress exponent n, the observed Q value can be greater than the diffusion activation energy when the pure metals and single-phase alloys are strengthened by fine precipitates [91]. The larger Q value was typical result found widely for power plant steels and other particle-strengthened alloys [86]. For example, the Q value was about 557 for EUROFER 97 and 625 KJ/mol.K for F82H-mod steels, respectively [86].

The obtained Q at the temperature range of 823 to 923 K with the constant stress of 220 MPa are shown in *Figs. 3-34* and *3-35* for JLF-1 and CLAM before ageing, respectively.

By linear regression analysis, the Q based on the equation 3-4 was about 456 and 426 KJ/mol.K for JLF-1 and CLAM, respectively. These values were higher than the self-diffusion energy of Fe (~300 KJ/mol.K), indicating the dislocation creep mechanism.

As a result, in the present study, the obtained activation energy (Q) together with stress exponent (n) indicated that the creep deformation was controlled by dislocation processes for the both steels.

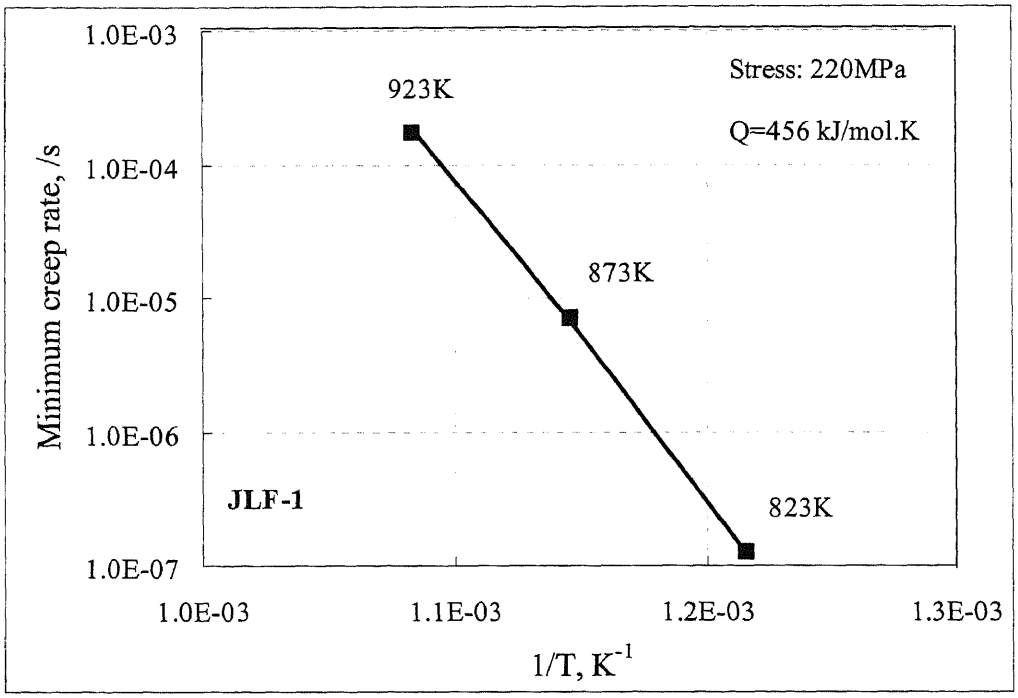

Fig. 3-34 The dependence of minimum creep rate on 1/T for JLF-1 before ageing, from which the activation energy Q of 456 kJ/mol-K was obtained.

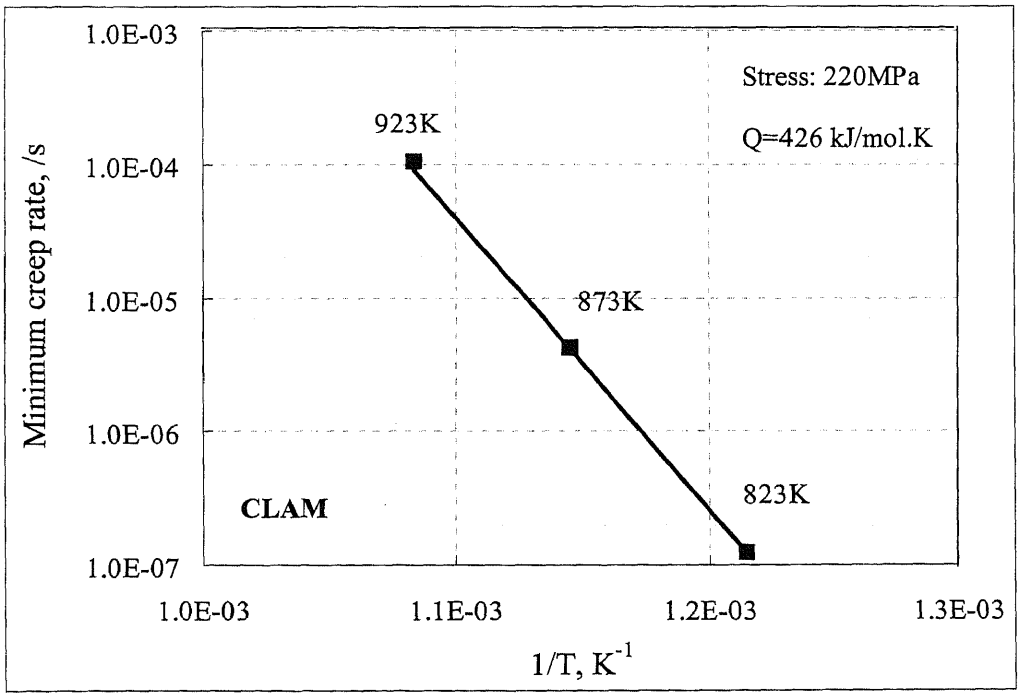

Fig. 3-35 The dependence of minimum creep rate on 1/T for CLAM before ageing, from which the activation energy Q of 426 kJ/mol-K was obtained.

3.5 Summary

1. The hardness increased slightly after ageing at 823 K up to 2000 h for JLF-1 and CLAM steels. However, ageing at higher than 823 K caused a decrease in hardness.
2. The tensile strength (yield strength and ultimate tensile strength) and total elongation did not change much after ageing at 823 K for 2000 h. However, ageing at higher than 823 K caused a decrease in tensile strength and corresponding increase in total elongation.
3. The creep properties (minimum creep rate and rupture time) improved after ageing at 823 and 873 K for 2000 h. However, the creep property degraded significantly after ageing at 973 K for 100 h when the applied stress was higher than 220 MPa.
4. The hardness, tensile and creep strength of CLAM were higher than those of JLF-1. However, these properties of CLAM were more susceptible to thermal ageing than those of JLF-1.
5. Based on Norton equation, the stress exponent n was almost constant at each test temperatures before and after ageing, suggesting unique creep mechanism during the present stress range. In addition, the obtained n was higher than the typical value of 3~5.
6. The activation energy Q was about 456 and 426 KJ/mol.K for JLF-1 and CLAM, respectively, which are higher than the self-diffusion activation energy of Fe (~300 KJ/mol.K). The obtained Q together with n indicated that the present steels were strengthened and the creep deformation was controlled by dislocation processes.